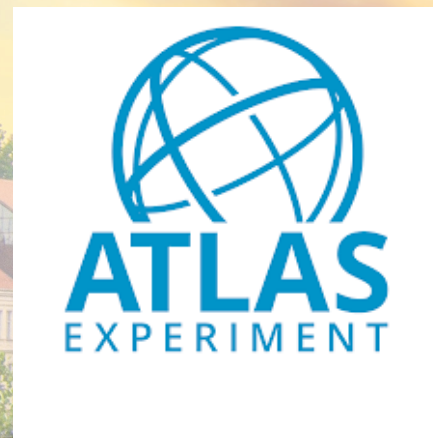


Higgs/Top/EWK and Global EFT results at ATLAS

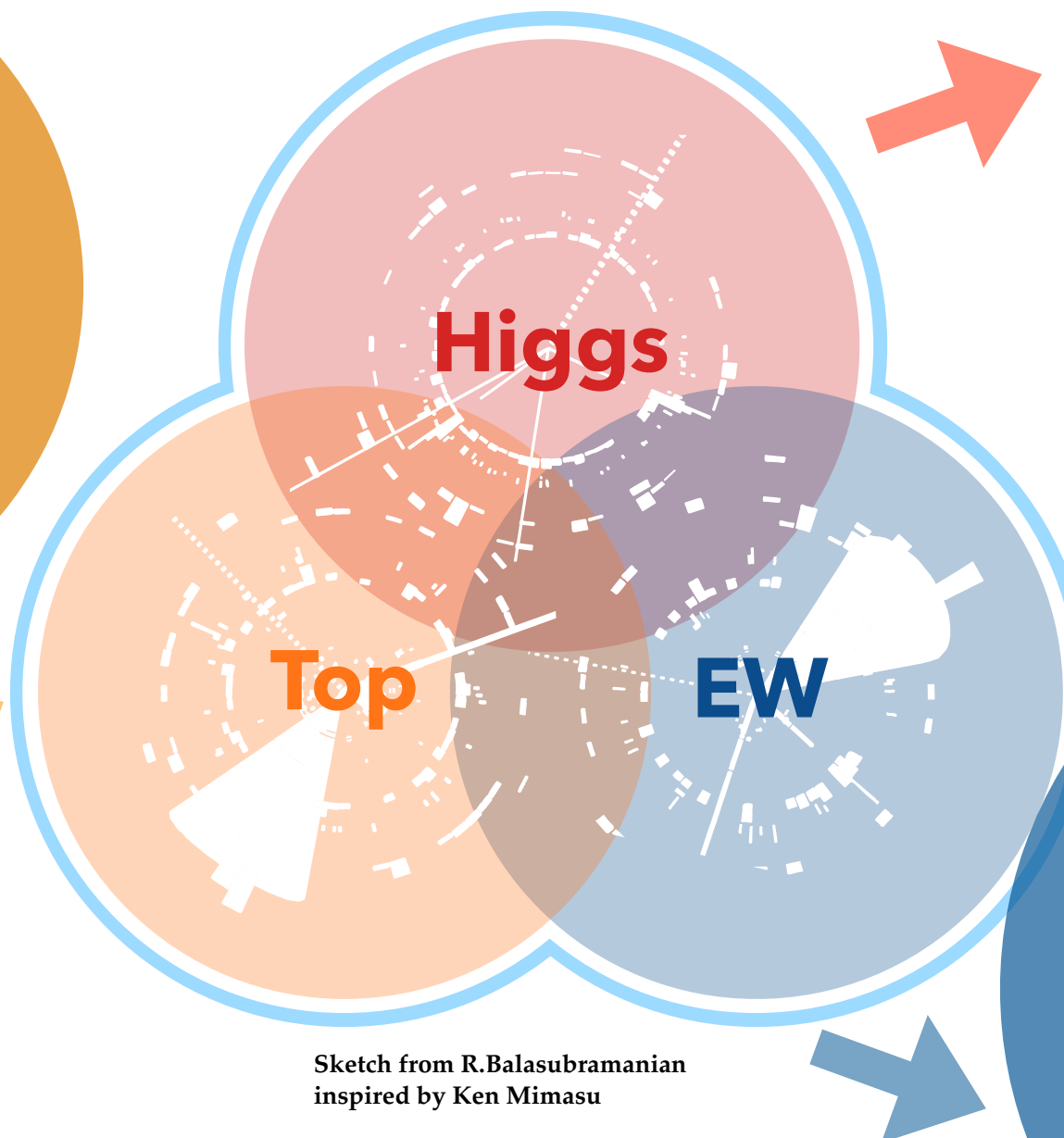
Eleonora Rossi

LHCP2023
22/05/2023

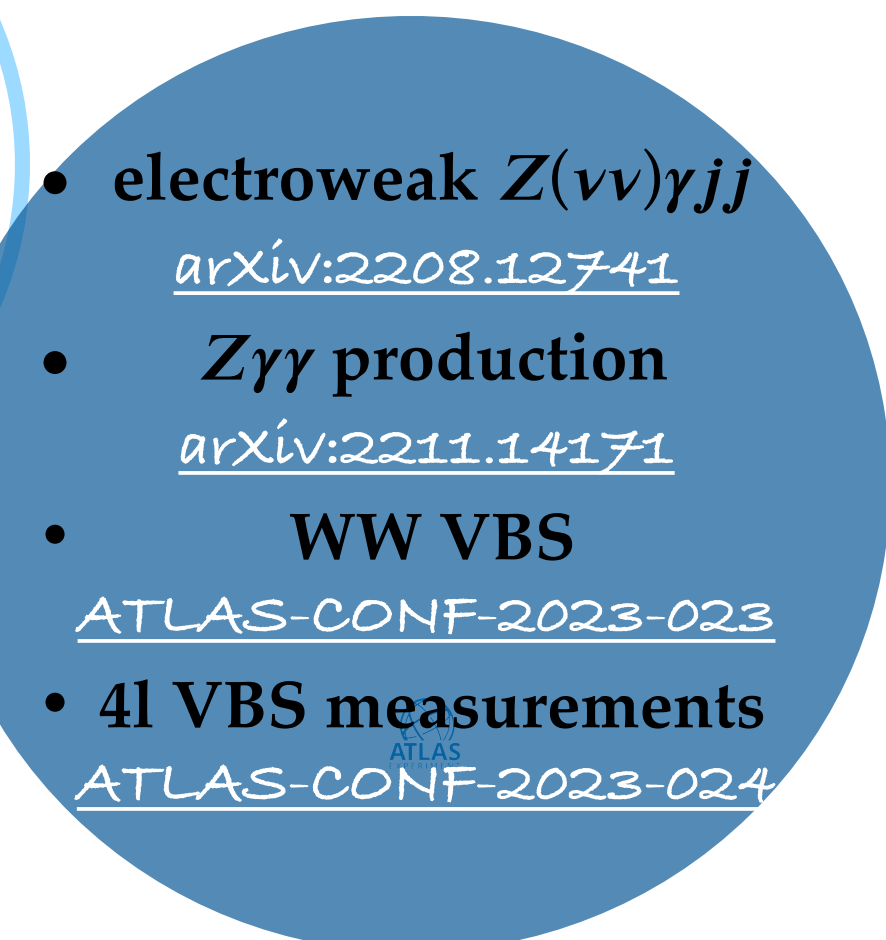


Latest results

- $t\bar{t}$ charge (rapidity) asymmetry:
[arXiv:2208.12095](https://arxiv.org/abs/2208.12095)
- 4 top observation
[arXiv:2303.15061](https://arxiv.org/abs/2303.15061)



- HH(4b) SMEFT + HEFT
[arXiv:2301.03212](https://arxiv.org/abs/2301.03212)



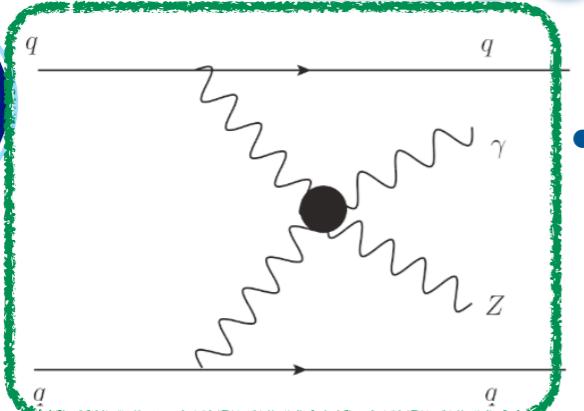
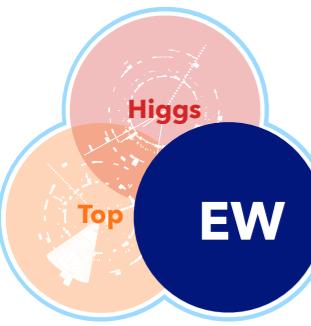
First ATLAS Global combination (Higgs+EW+EWPO):

[ATL-PHYS-PUB-2022-037](https://cds.cern.ch/record/2903427)

(SMEFTsim + SMEFT@NLO)

Electroweak Z($\nu\nu$) γjj

[arxiv:2208.12741](https://arxiv.org/abs/2208.12741)

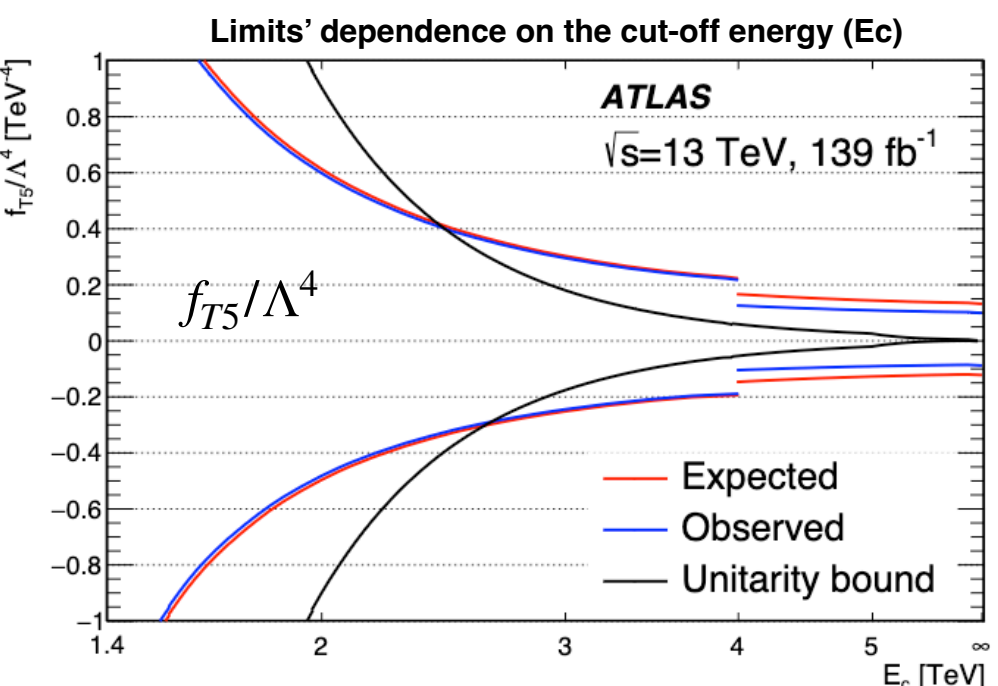
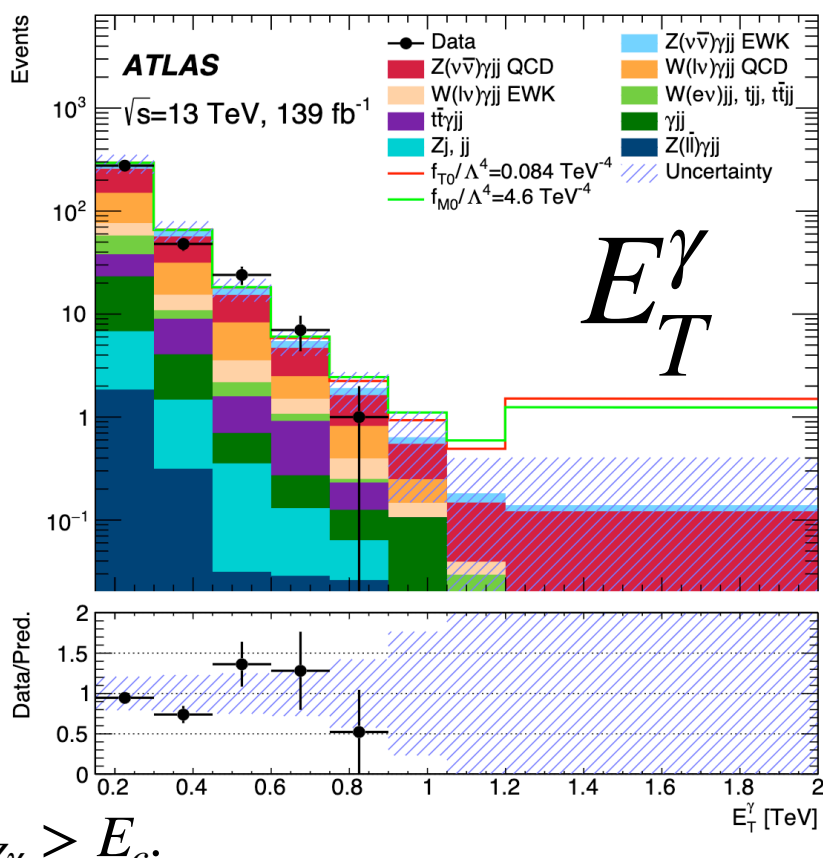


- Measurement of the **fiducial cross section** for EWK $Z(\bar{\nu}\nu)\gamma jj$ in the region of $E_T^\gamma > 150$ GeV - **first evidence!!!**

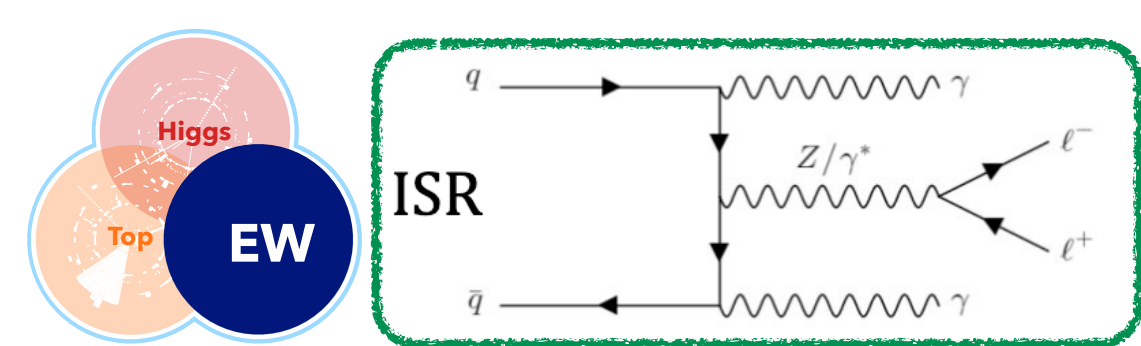
- BSM physics could induce anomalous QGCs, enhancing the **cross section** and modifying the **kinematic distributions** of the final-state bosons.
- The effect of new physics introduced by aQGCs can be realised using an EFT linearly parameterised by an effective Lagrangian.
- A clipping technique is introduced to preserve unitarity at very high parton centre-of-mass energies: the anomalous signal contribution is set to zero for $m_{Z\gamma} > E_c$.

one at a time limits; unitarity is not preserved

Coefficient	Observed limit [TeV $^{-4}$]	Expected limit [TeV $^{-4}$]
f_{T0}/Λ^4	$[-9.4, 8.4] \times 10^{-2}$	$[-1.3, 1.2] \times 10^{-1}$
f_{T5}/Λ^4	$[-8.8, 9.9] \times 10^{-2}$	$[-1.2, 1.3] \times 10^{-1}$
f_{T8}/Λ^4	$[-5.9, 5.9] \times 10^{-2}$	$[-8.1, 8.0] \times 10^{-2}$
f_{T9}/Λ^4	$[-1.3, 1.3] \times 10^{-1}$	$[-1.7, 1.7] \times 10^{-1}$
f_{M0}/Λ^4	$[-4.6, 4.6]$	$[-6.2, 6.2]$
f_{M1}/Λ^4	$[-7.7, 7.7]$	$[-1.0, 1.0] \times 10^1$
f_{M2}/Λ^4	$[-1.9, 1.9]$	$[-2.6, 2.6]$



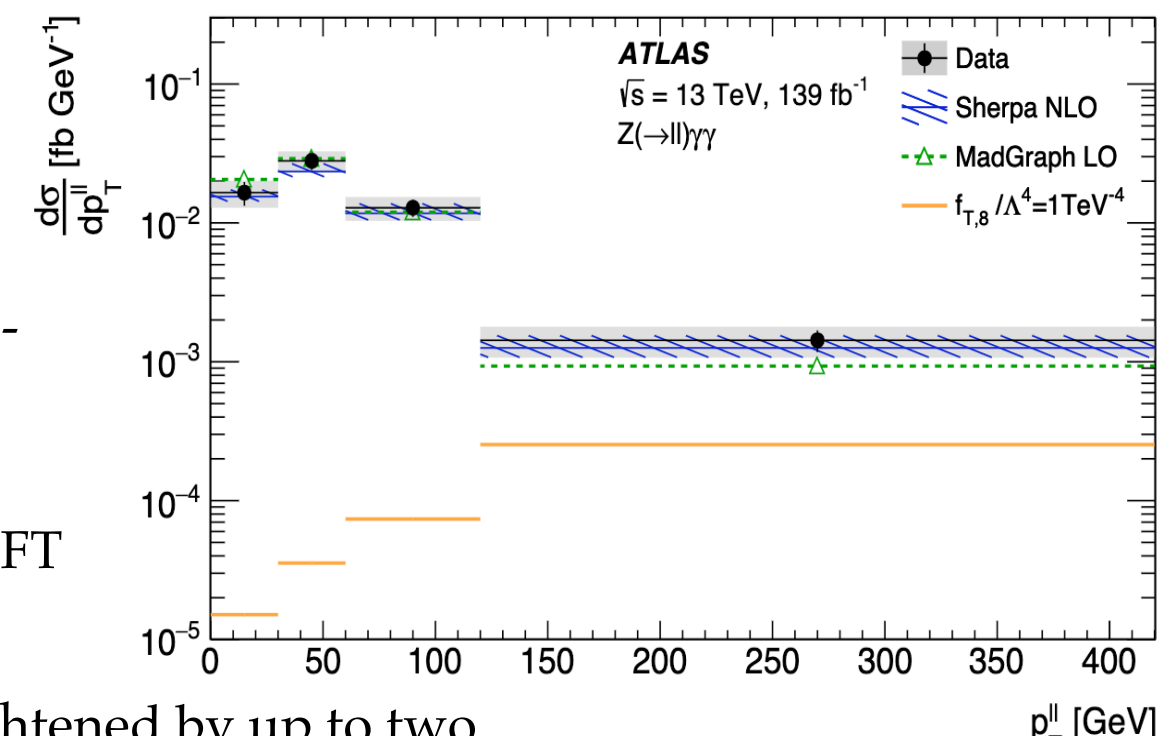
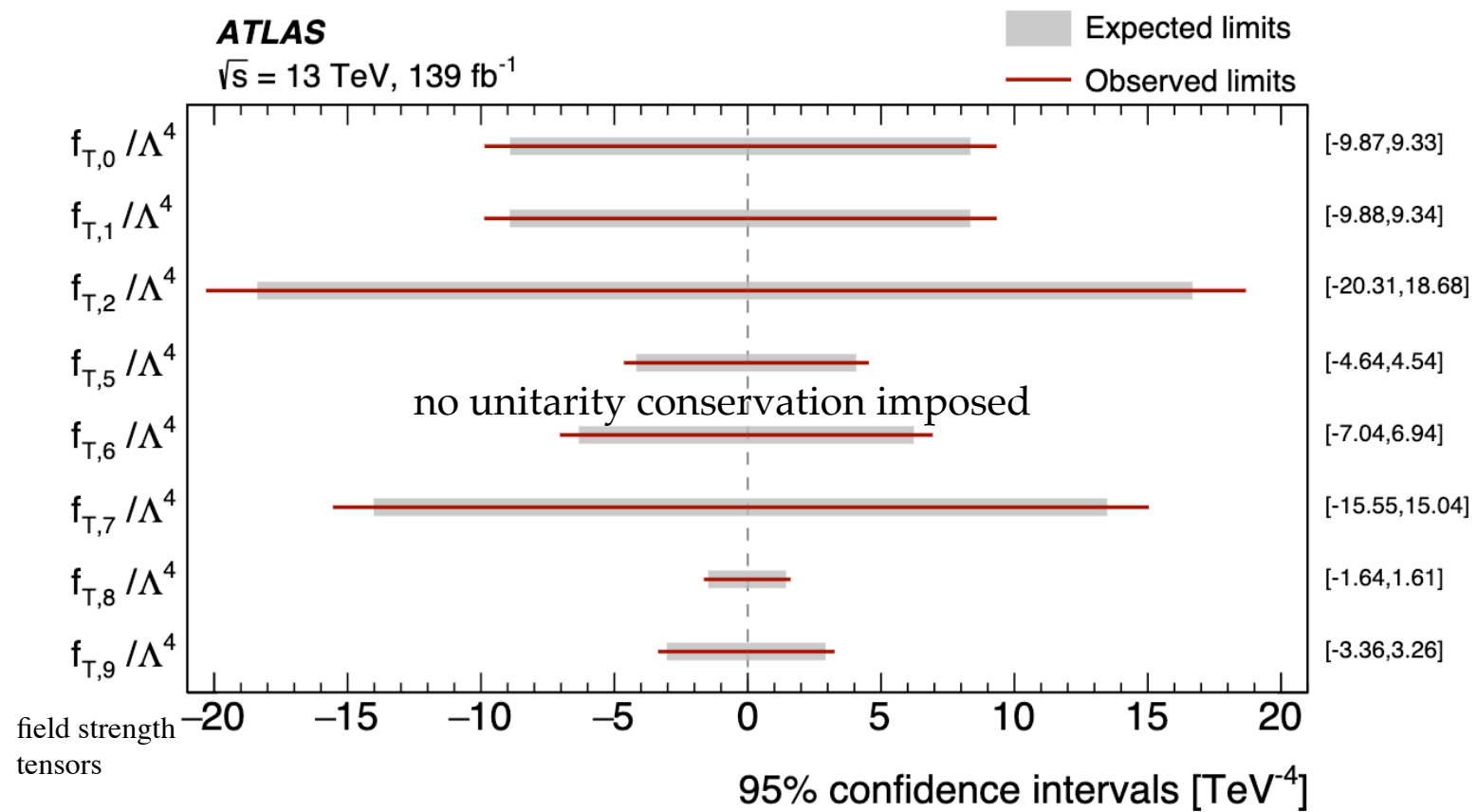
- Constraints on EFT coefficients are either competitive with or more stringent than those previously published by CMS.
- The constraints on $f_{T5}/\Lambda^4, f_{T8}/\Lambda^4$ and f_{T9}/Λ^4 are significantly stronger than results previously published by ATLAS and CMS.



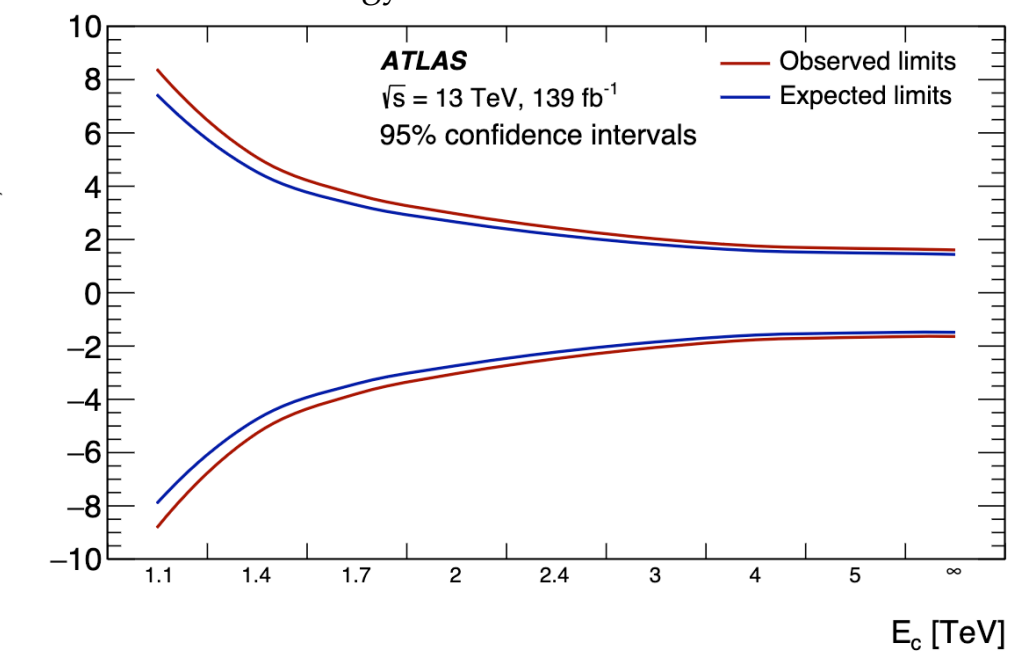
Z $\gamma\gamma$ production

[arXiv:2211.14171](https://arxiv.org/abs/2211.14171)

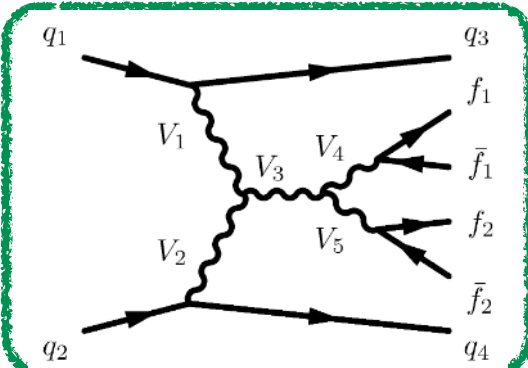
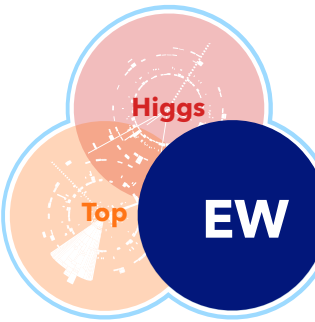
- Production of a Z boson in association with two photons in a phase-space region dominated by the ISR production of photons.
- Integrated and differential cross-sections** measured (first time - differential).
- Sensitive to transverse operators involving neutral aQGCs.
- $p_T^{\ell\ell}$ **unfolded cross-section** used to set limits on dim8 WCs in EFT framework as it is the most sensitive to NP effects.
- The constraints on four of the eight operators considered are tightened by up to two orders of magnitude with respect to previous ATLAS analyses using 8 TeV data.



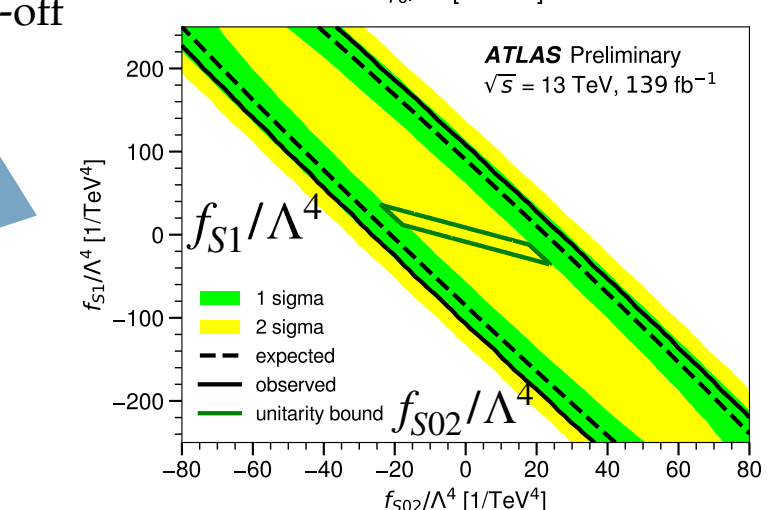
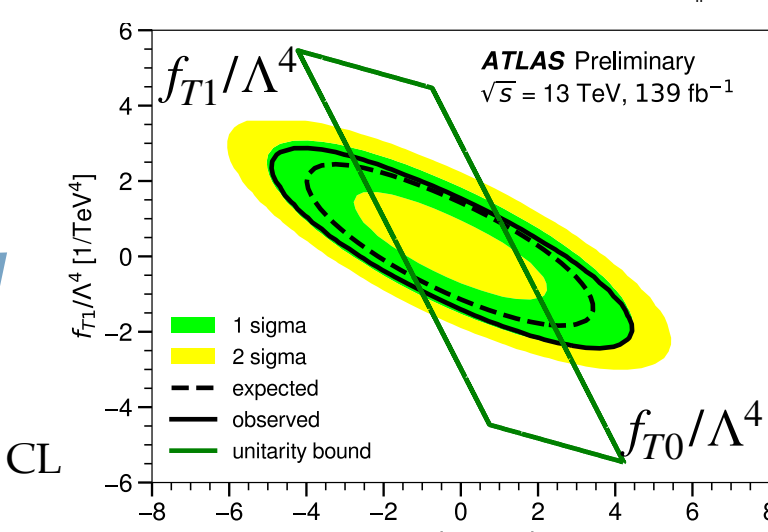
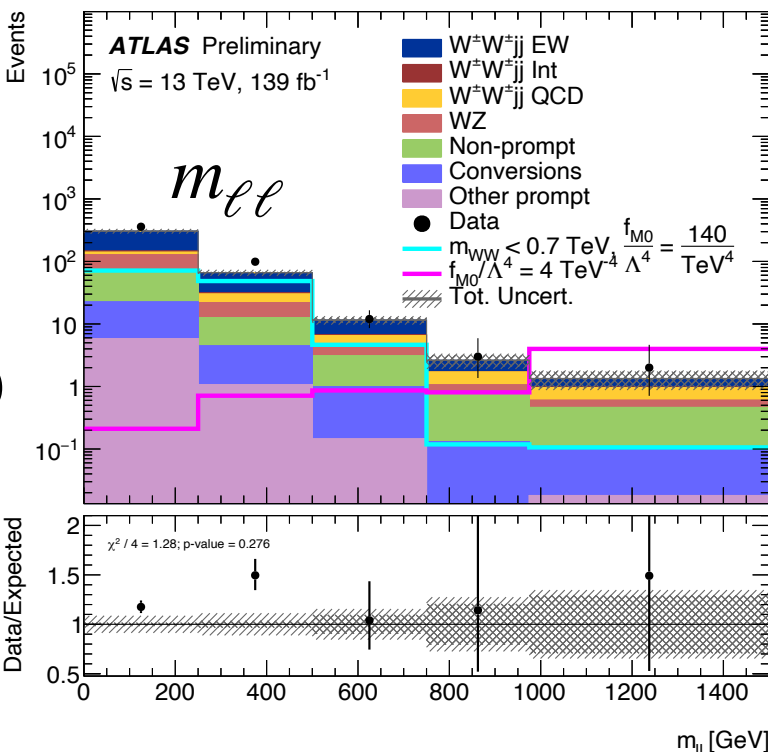
- clipping approach - EFT contribution is suppressed above an energy scale E_c .



WW VBS



ATLAS-CONF-2023-023



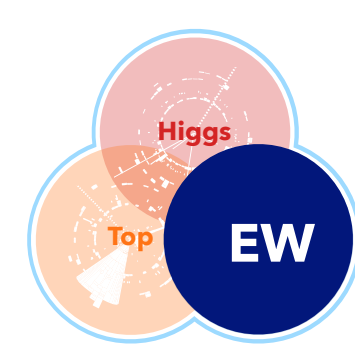
- Fiducial and differential cross sections for the electroweak and inclusive production of a same-sign W boson pair in association with two jets ($W\pm W\pm j j$)
- (analysis details in Alessandro's talk).
- Differential $m_{\ell\ell}$ distribution with optimised binning used to set limits on EFT dim8 operator coefficients $f_{S02}/\Lambda^4, f_{S1}/\Lambda^4, f_{M0}/\Lambda^4, f_{M1}/\Lambda^4, f_{M7}/\Lambda^4, f_{T0}/\Lambda^4, f_{T1}/\Lambda^4$, and f_{T2}/Λ^4 .
- Results using EFT unitarisation cut-off also provided.
- Constraints competitive with those previously published by CMS.

Three families of operators (M, S - covariant derivative, T)

Coefficient	Type	No unitarisation cut-off	Lower and upper limit at the respective unitarity bound
		[TeV $^{-4}$]	[TeV $^{-4}$]
f_{M0}/Λ^4	exp.	[-3.9, 3.8]	-64 at 0.9 TeV, 40 at 1.0 TeV
	obs.	[-4.1, 4.1]	-140 at 0.7 TeV, 117 at 0.8 TeV
f_{M1}/Λ^4	exp.	[-6.3, 6.6]	-25.5 at 1.6 TeV, 31 at 1.5 TeV
	obs.	[-6.8, 7.0]	-45 at 1.4 TeV, 54 at 1.3 TeV
f_{M7}/Λ^4	exp.	[-9.3, 8.8]	-33 at 1.8 TeV, 29.1 at 1.8 TeV
	obs.	[-9.8, 9.5]	-39 at 1.7 TeV, 42 at 1.7 TeV
f_{S02}/Λ^4	exp.	[-5.5, 5.7]	-94 at 0.8 TeV, 122 at 0.7 TeV
	obs.	[-5.9, 5.9]	-
f_{S1}/Λ^4	exp.	[-22.0, 22.5]	-
	obs.	[-23.5, 23.6]	-
f_{T0}/Λ^4	exp.	[-0.34, 0.34]	-3.2 at 1.2 TeV, 4.9 at 1.1 TeV
	obs.	[-0.36, 0.36]	-7.4 at 1.0 TeV, 12.4 at 0.9 TeV
f_{T1}/Λ^4	exp.	[-0.158, 0.174]	-0.32 at 2.6 TeV, 0.44 at 2.4 TeV
	obs.	[-0.174, 0.186]	-0.38 at 2.5 TeV, 0.49 at 2.4 TeV
f_{T2}/Λ^4	exp.	[-0.56, 0.70]	-2.60 at 1.7 TeV, 10.3 at 1.2 TeV
	obs.	[-0.63, 0.74]	-

2D limits at 95% CL
obtained with a
unitarisation cut-off
scale of 1.5 TeV





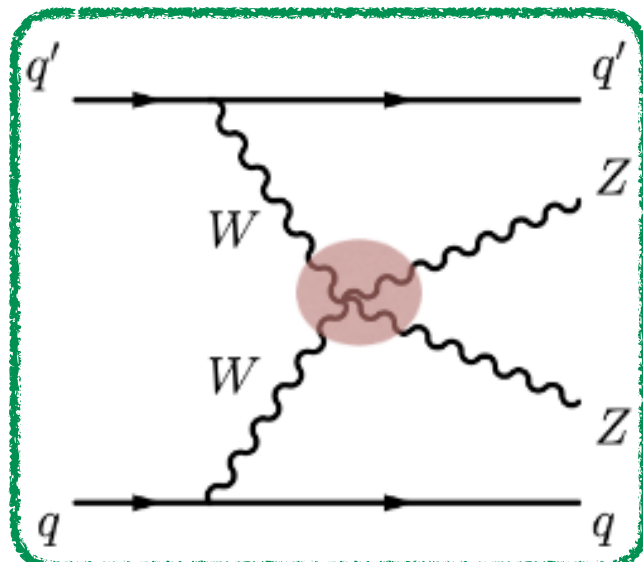
41 VBS measurements

ATLAS-CONF-2023-024

- Differential cross-sections ($m_{4\ell}$ and m_{jj}) measured for the production of four charged leptons in association with two jets (analysis details in [Chilufya's talk](#)).

- Unfolded cross sections used to search for signatures of anomalous weak-boson self-interactions using the framework of dim8 EFT.

$$\mathcal{O}_{T0}, \mathcal{O}_{T1}, \mathcal{O}_{T2}, \mathcal{O}_{T5}, \mathcal{O}_{T6}, \mathcal{O}_{T7}, \mathcal{O}_{T8}, \mathcal{O}_{T9}$$

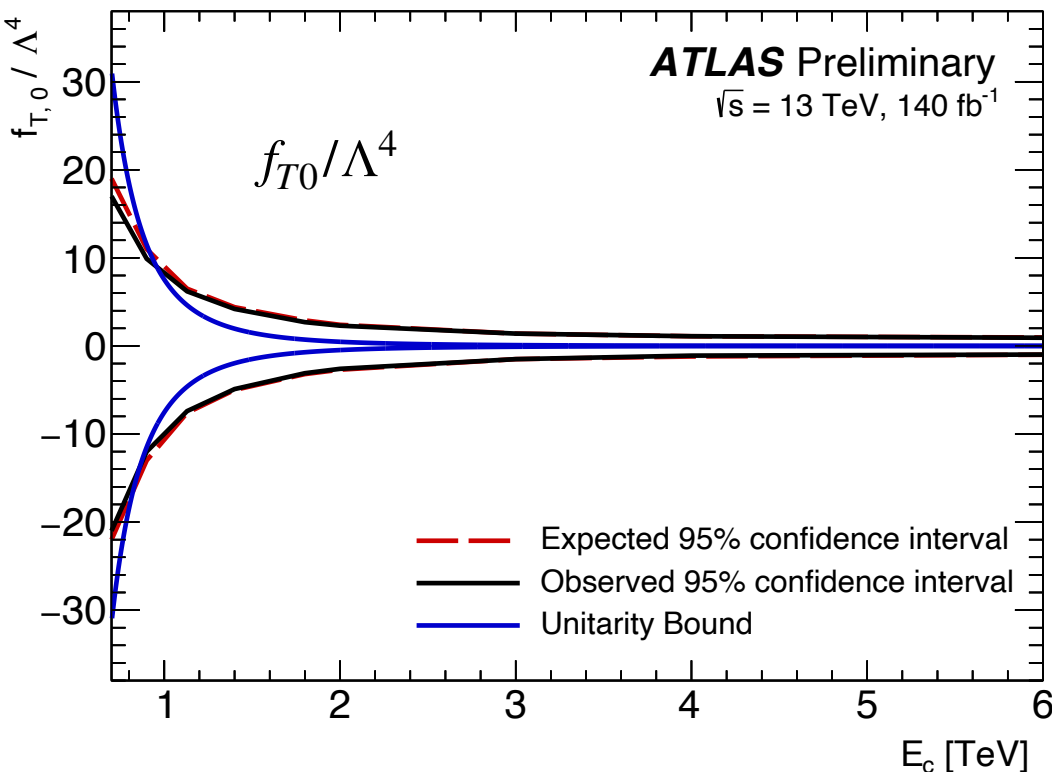


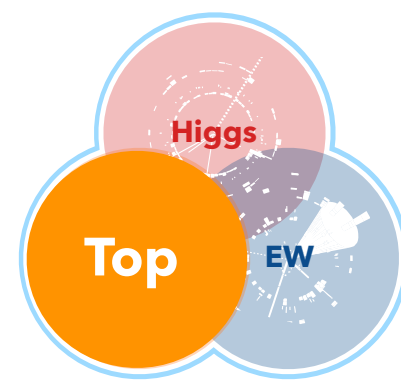
- The WCs associated with the \mathcal{O}_{T0} and \mathcal{O}_{T1} operators are the most tightly constrained.
- Constraints with the pure dim8 contribution are more stringent than interference-only constraints.

field strength
tensors

Wilson coefficient	$ \mathcal{M}_{d8} ^2$	95% confidence interval [TeV $^{-4}$]	
	Included	Expected	Observed
$f_{T,0}/\Lambda^4$	yes	[-0.98, 0.93]	[-1.0, 0.97]
	no	[-23, 17]	[-19, 19]
$f_{T,1}/\Lambda^4$	yes	[-1.2, 1.2]	[-1.3, 1.3]
	no	[-160, 120]	[-140, 140]
$f_{T,2}/\Lambda^4$	yes	[-2.5, 2.4]	[-2.6, 2.5]
	no	[-74, 56]	[-63, 62]
$f_{T,5}/\Lambda^4$	yes	[-2.5, 2.4]	[-2.6, 2.5]
	no	[-79, 60]	[-68, 67]
$f_{T,6}/\Lambda^4$	yes	[-3.9, 3.9]	[-4.1, 4.1]
	no	[-64, 48]	[-55, 54]
$f_{T,7}/\Lambda^4$	yes	[-8.5, 8.1]	[-8.8, 8.4]
	no	[-260, 200]	[-220, 220]
$f_{T,8}/\Lambda^4$	yes	[-2.1, 2.1]	[-2.2, 2.2]
	no	$[-4.6, 3.1] \times 10^4$	$[-3.9, 3.8] \times 10^4$
$f_{T,9}/\Lambda^4$	yes	[-4.5, 4.5]	[-4.7, 4.7]
	no	$[-7.5, 5.5] \times 10^4$	$[-6.4, 6.3] \times 10^4$

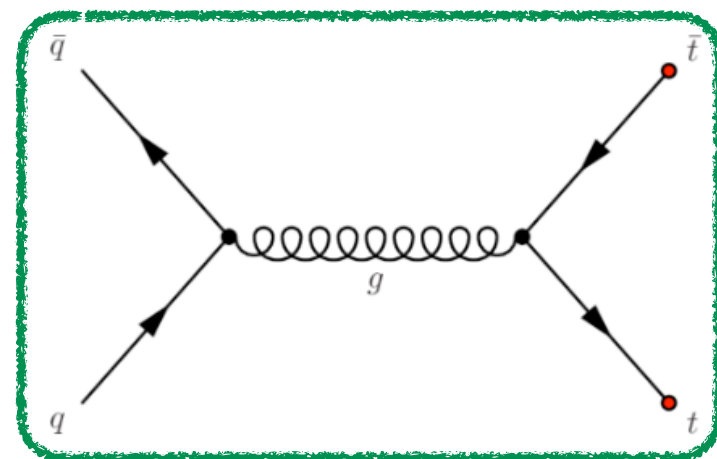
- Constraints are placed on each WC after restricting the interference- and pure dimension-eight contributions to have $m_{4\ell} < E_c$
- The 95% confidence intervals degrade by a factor of 4-5 ($E_c = \infty$ to $E_c = 1$ TeV).





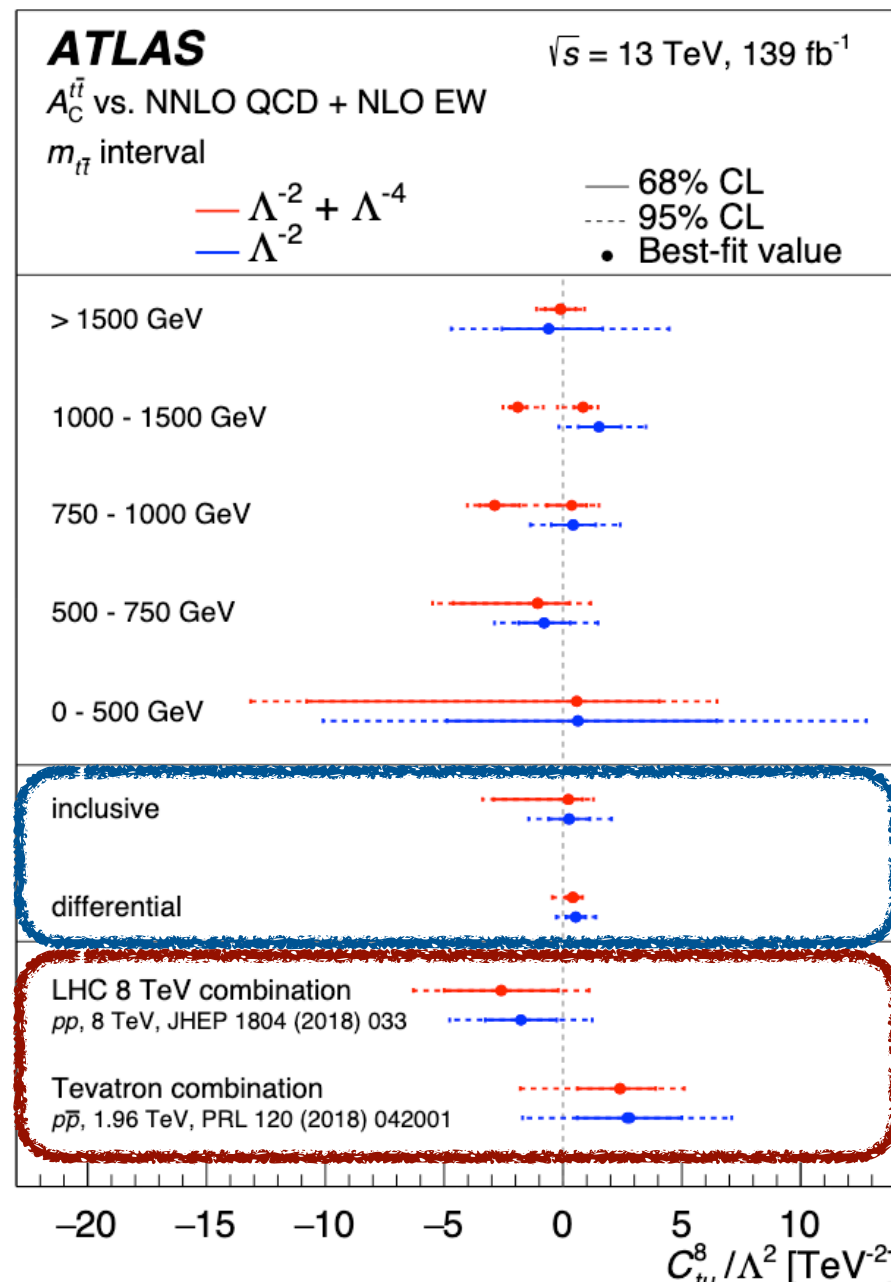
Evidence for the charge asymmetry in $pp \rightarrow t\bar{t}$

[arXiv:2208.12095](https://arxiv.org/abs/2208.12095)



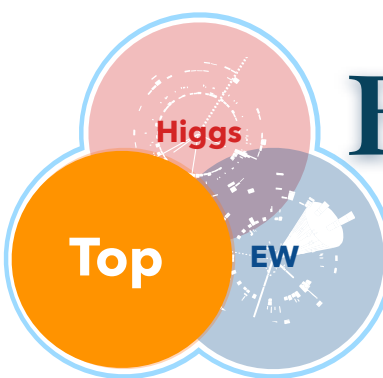
- Inclusive and differential measurement of $t\bar{t}$ and leptonic charge asymmetry $A_c^{t\bar{t}}$ & $A_c^{\ell\bar{\ell}}$ with full Run2 dataset.
- Differential measurements provided for invariant mass, transverse momentum and longitudinal boost of the $t\bar{t}$ system.
- $A_c^{t\bar{t}}$ results are interpreted in the SMEFT framework (SMEFT@NLO).
- 14 four-fermion operators** + 1 operator for top–gluon interaction.

- Large improvement w.r.t LHC 8 TeV / Tevatron results
- Interplay between EFT sensitivity (increases for higher $m_{t\bar{t}}$) and statistical uncertainty (0.2% – 0.3% to 2.9%).
- Tightest limit obtained for the linear EFT approximation in the mass bin from 1 to 1.5 TeV.
- Constraint from the differential $A_c^{t\bar{t}}$ measurement more than a factor 2 stronger than inclusive measurement.



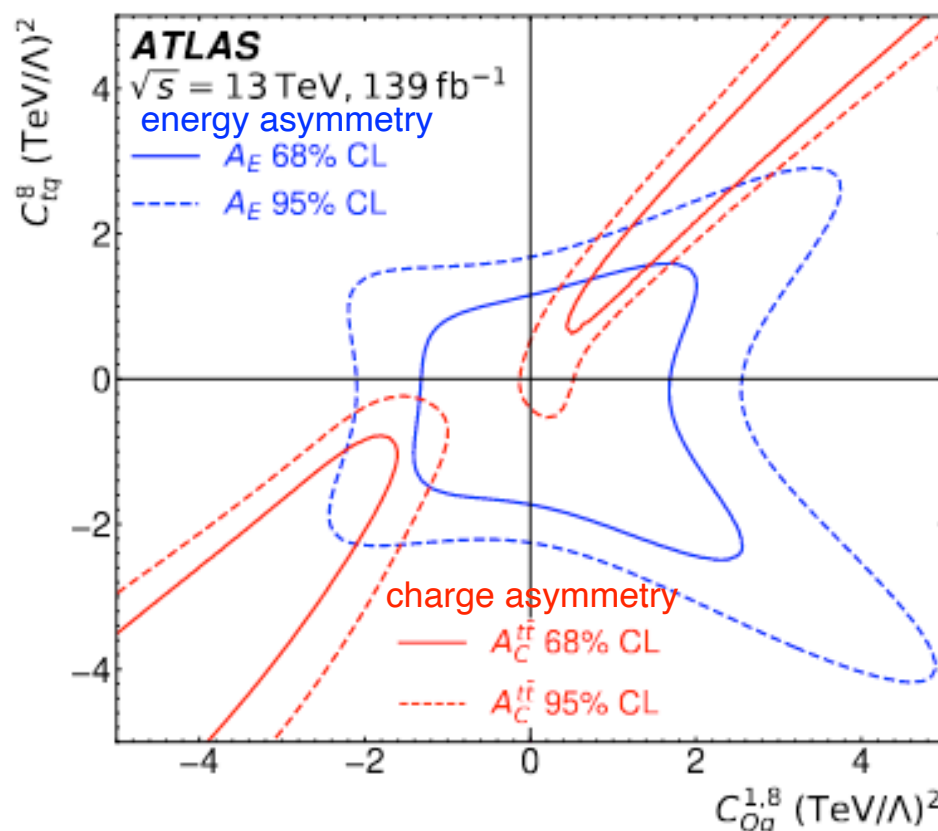
The combined inclusive charge asymmetry is measured to be $A_c^{t\bar{t}} = 0.0068 \pm 0.0015$, which differs from zero by **4.7 standard deviations**.

Evidence for the charge asymmetry in $pp \rightarrow t\bar{t}$



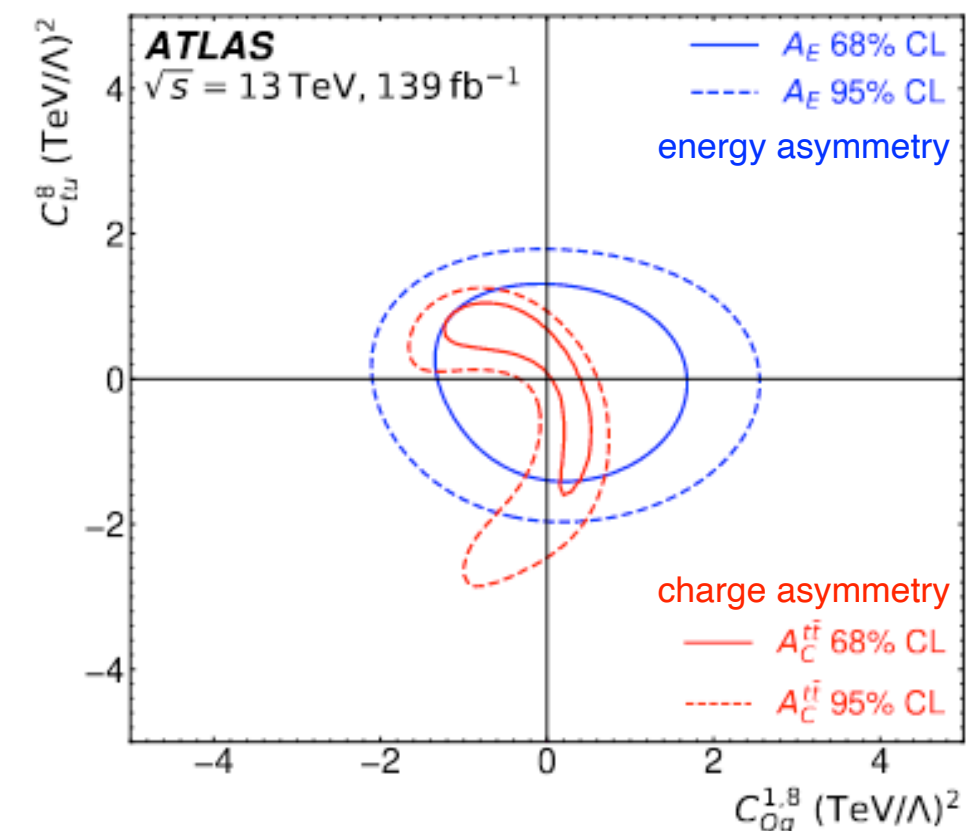
[arXiv:2208.12095](https://arxiv.org/abs/2208.12095)

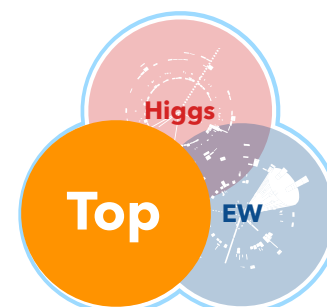
- The obtained EFT bounds (from charge asymmetry) are compared to those from energy asymmetry measurement in $t\bar{t}j$ production. [Energy Asymmetry](#)
- QCD structure of the energy asymmetry is different due to the extra jet in $t\bar{t}j$ production.
 - the two asymmetries probe different directions in chiral and colour space.
- Different shapes of the bounds for colour-octet operators with the same chirality scenarios:
 - charge asymmetry (dashed/solid red lines) leaves a blind direction broken by the energy asymmetry (dashed/solid blue lines) due to operator interference with the QCD amplitude.



blind direction for
charge
asymmetry broken
using
energy asymmetry
measurement

Bounds on color-octet
operators

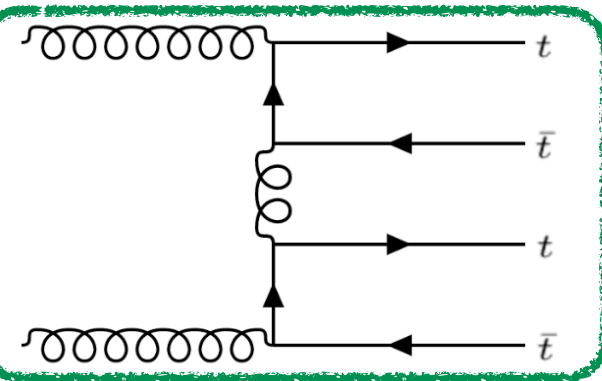




4 top observation

[arXiv:2303.15061](https://arxiv.org/abs/2303.15061)

Accepted for journal publication

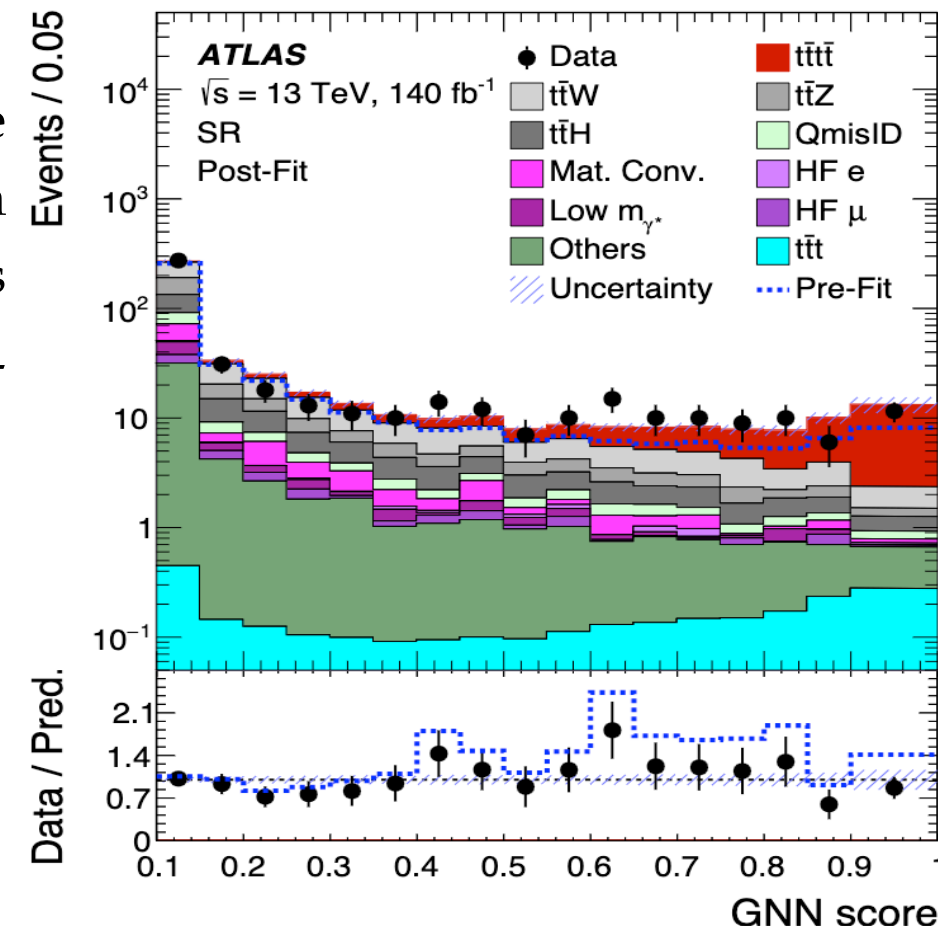


- The $t\bar{t}t\bar{t}$ process (**observed** with a significance of 6.1σ) is sensitive to 4 heavy-flavour fermion operators, $O_{tt}^1, O_{QQ}^1, O_{Qt}^1, O_{Qt}^8 \rightarrow$ BSM models that enhance interactions between the third-generation quarks (Johnny's talk).
- Limits on EFT parameters extracted parameterising the $t\bar{t}t\bar{t}$ yield in each bin of the multivariate discriminant score distribution (used to separate signal and background).

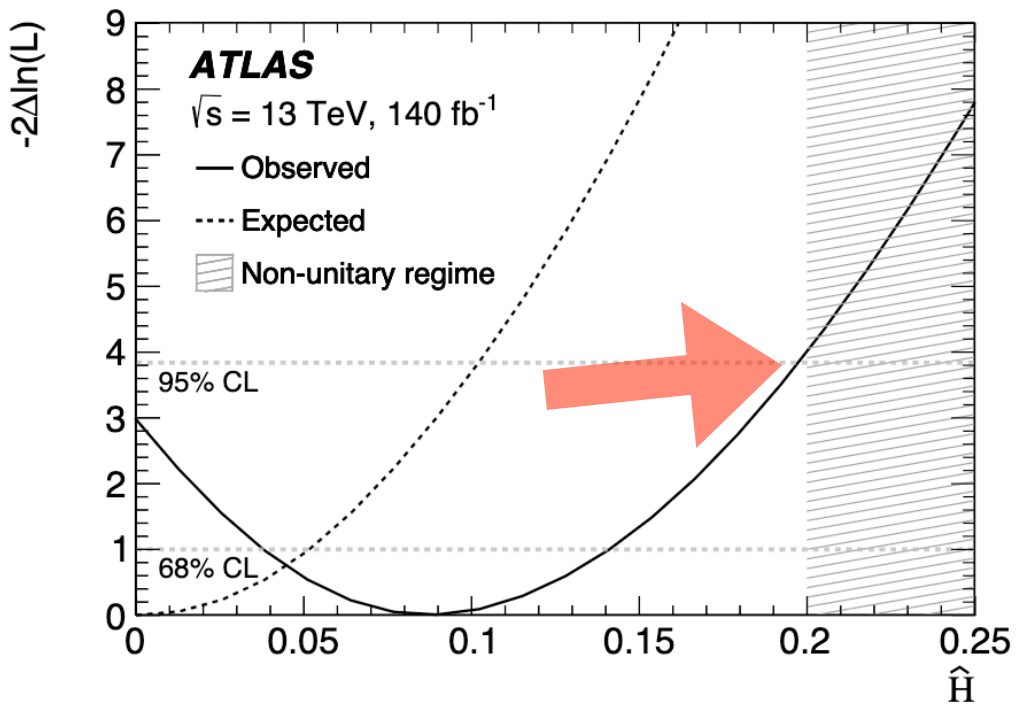
other WCs are fixed to SM, linear+quadratic terms included

Operators	Expected $C_i/\Lambda^2 [\text{TeV}^{-2}]$	Observed $C_i/\Lambda^2 [\text{TeV}^{-2}]$
O_{QQ}^1	[-2.4, 3.0]	[-3.5, 4.1]
O_{Qt}^1	[-2.5, 2.0]	SMEFT@NLO [-3.5, 3.0]
O_{tt}^1	[-1.1, 1.3]	[-1.7, 1.9]
O_{Qt}^8	[-4.2, 4.8]	[-6.2, 6.9]

- Limits on the Higgs oblique parameter, \hat{H} , defined as the Wilson coefficient of the sole dim6 operator that affects the off-shell Higgs interaction ($t\bar{t}t\bar{t}$ cross section + $t\bar{t}H$ background production), are set.
- Observed upper limit at 95% CL on $\hat{H}=0.20$:**
 - coincides with the largest value that still preserves unitarity.

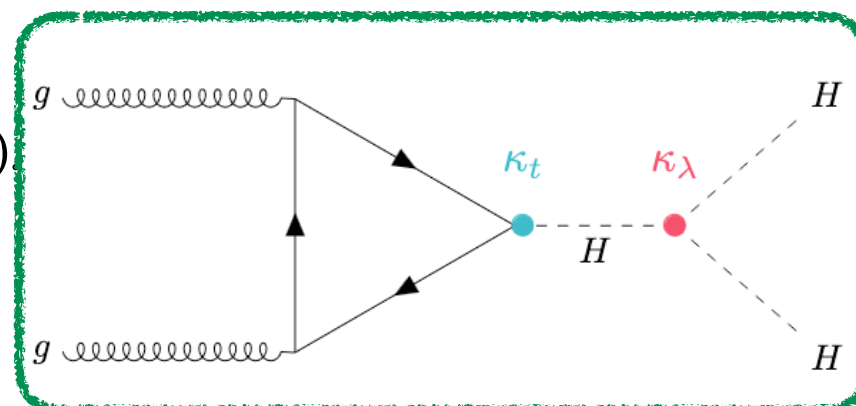


Leading uncertainties: signal modeling uncertainties, statistical uncertainty



- Non-resonant HH ggF production - 4b decay channel (126 fb^{-1}).
- Analysis categorisations to improve sensitivity to BSM physics.

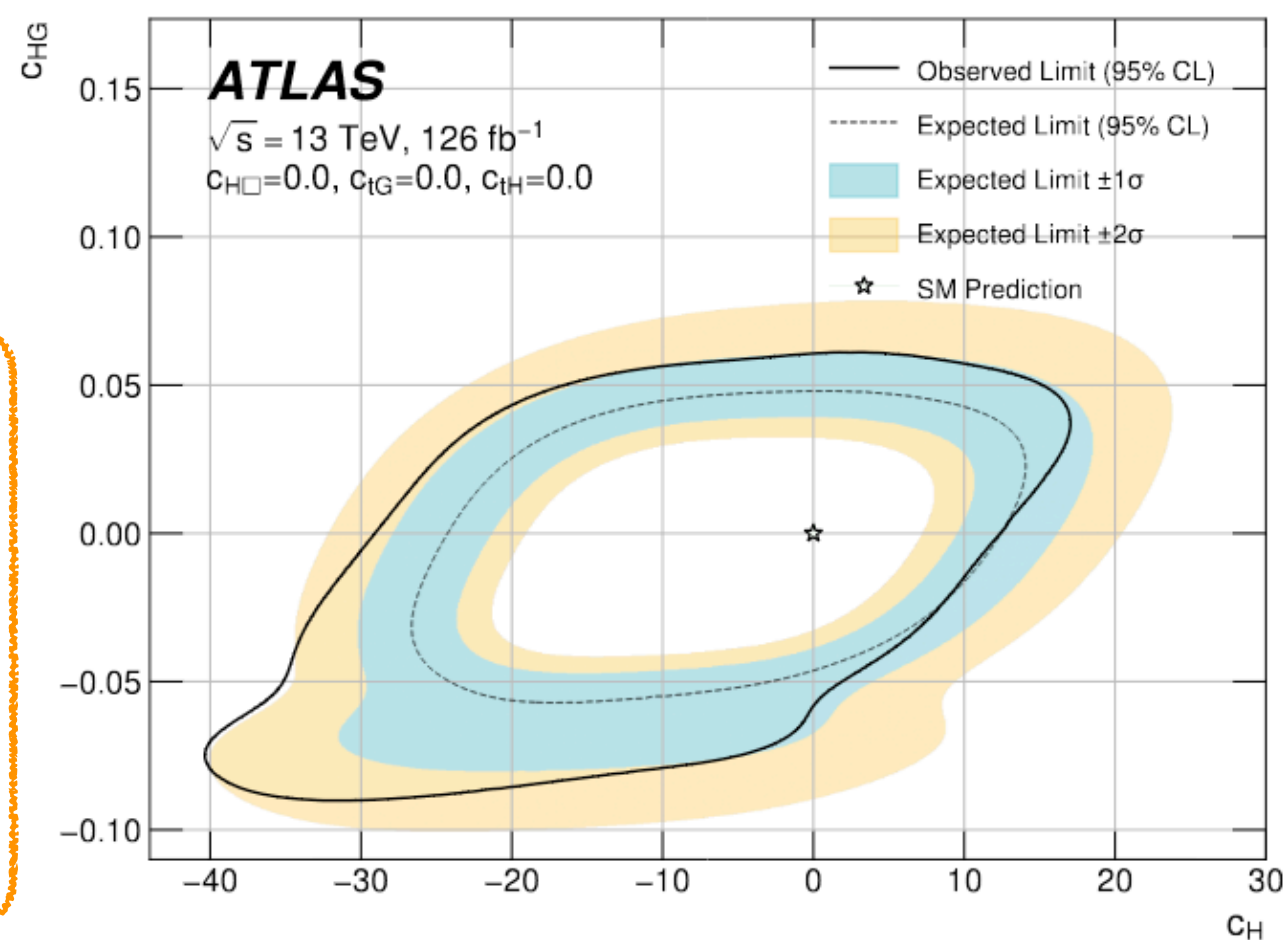
- The interpretations are performed with two EFT frameworks, Higgs Effective Field Theory (HEFT) and SM Effective Field Theory (SMEFT).
- first LHC SMEFT interpretation for HH.
- The different BSM scenarios are considered re-weighting the SM non-resonant HH ggF sample.



- 1D and 2D limits for the 5 Wilson coefficients: $c_H, c_{H\square}, c_{tH}, c_{tG}, c_{HG}$. SMEFT@NLO

linear+quadratic results, one WC at a time

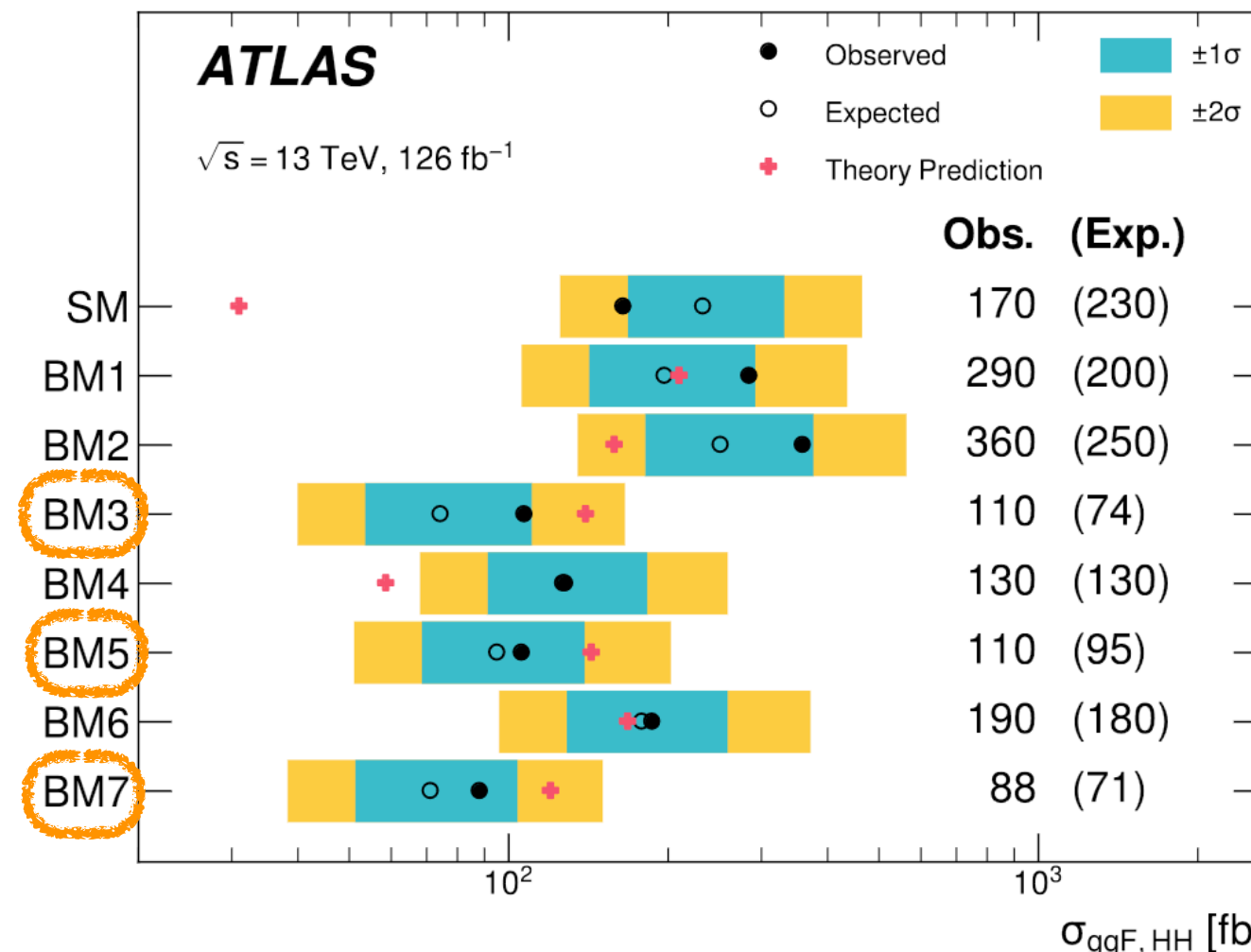
Parameter	Expected Constraint		Observed Constraint	
	Lower	Upper	Lower	Upper
c_H	-20	11	-22	11
c_{HG}	-0.056	0.049	-0.067	0.060
$c_{H\square}$	-9.3	13.9	-8.9	14.5
c_{tH}	-10.0	6.4	-10.7	6.2
c_{tG}	-0.97	0.94	-1.12	1.15



Other 2D scans in backup



- 7 HEFT benchmark models for c_{HHH} , c_{ttH} , c_{ttHH} , c_{ggH} and c_{ggHH} to probe a wide variety of characteristic shapes of the m_{HH} spectrum.
- Advantage of HEFT: anomalous single-Higgs-boson and HH couplings defined separately.
- The spread of sensitivity between the seven benchmark models reflects the different shapes of the signal m_{HH} distributions.
- BM3, BM5 and BM7 are observed to be excluded with more than 95% confidence.



- Limits competitive with ATLAS $b\bar{b}\tau\tau + b\bar{b}\gamma\gamma$ standalone limits \rightarrow improvement when included in the combination

$HH \rightarrow b\bar{b}b\bar{b}$

c_{gghh}	[-0.36,0.78] [-0.42,0.75]	
$c_{t\bar{t}HH}$	[-0.55,0.51] [-0.46,0.40]	

$HH \rightarrow b\bar{b}\tau\tau + b\bar{b}\gamma\gamma$

Wilson coefficient	Combination	
	Obs.	Exp.
c_{gghh}	[-0.3, 0.4]	[-0.3, 0.3]
$c_{t\bar{t}hh}$	[-0.2, 0.6]	[-0.2, 0.6]

The different variation between observed and expected limits is linked to a slight excess observed in the low m_{HH} region

[ATL-PHYS-PUB-2022-019](https://cds.cern.ch/record/2922219)



ATLAS Global combination

SMEFT interpretation (SMEFTsim and SMEFTatNLO)

ATL-PHYS-PUB-2022-037

Decay channel	Target Production Modes	\mathcal{L} [fb $^{-1}$]
$H \rightarrow \gamma\gamma$	ggF, VBF, WH, ZH, $t\bar{t}H$, tH	139
$H \rightarrow ZZ^*$	ggF, VBF, WH, ZH, $t\bar{t}H(4\ell)$	139
$H \rightarrow WW^*$	ggF, VBF	139
$H \rightarrow \tau\tau$	ggF, VBF, WH, ZH, $t\bar{t}H(\tau_{\text{had}}\tau_{\text{had}})$	139
	WH, ZH	139
$H \rightarrow b\bar{b}$	VBF	126
	$t\bar{t}H$	139

- ATLAS Higgs boson data (2021 combination)
 - Higgs boson production and decay combined measurements in STXS bins
- Higgs Combination

Process	Important phase space requirements	Observable	\mathcal{L} [fb $^{-1}$]
$pp \rightarrow e^\pm \nu \mu^\mp \nu$	$m_{\ell\ell} > 55 \text{ GeV}$, $p_T^{\text{jet}} < 35 \text{ GeV}$	$p_T^{\text{lead. lep.}}$	36
$pp \rightarrow \ell^\pm \nu \ell^\pm \ell^-$	$m_{\ell\ell} \in (81, 101) \text{ GeV}$	m_T^{WZ}	36
$pp \rightarrow \ell^+ \ell^- \ell^+ \ell^-$	$m_{4\ell} > 180 \text{ GeV}$	m_{Z2}	139
$pp \rightarrow \ell^+ \ell^- jj$	$m_{jj} > 1000 \text{ GeV}$, $m_{\ell\ell} \in (81, 101) \text{ GeV}$	$\Delta\phi_{jj}$	139

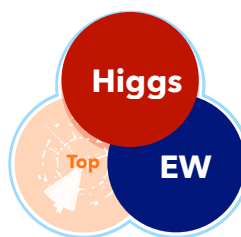
WW,WZ,4l, Z+2jets combination

- ATLAS electroweak data
- Differential cross-section measurements for diboson and Z production via VBF

Observable	Measurement	Prediction	Ratio
Γ_Z [MeV]	2495.2 ± 2.3	2495.7 ± 1	0.9998 ± 0.0010
R_ℓ^0	20.767 ± 0.025	20.758 ± 0.008	1.0004 ± 0.0013
R_c^0	0.1721 ± 0.0030	0.17223 ± 0.00003	0.999 ± 0.017
R_b^0	0.21629 ± 0.00066	0.21586 ± 0.00003	1.0020 ± 0.0031
$A_{\ell,\ell}^{0,\ell}$	0.0171 ± 0.0010	0.01718 ± 0.00037	0.995 ± 0.062
$A_{c,c}^{0,c}$	0.0707 ± 0.0035	0.0758 ± 0.0012	0.932 ± 0.048
$A_{b,b}^{0,b}$	0.0992 ± 0.0016	0.1062 ± 0.0016	0.935 ± 0.021
σ_{had}^0 [pb]	41488 ± 6	41489 ± 5	0.99998 ± 0.00019

Precision Electroweak Measurements on the Z Resonance

- Electroweak precision observables measured at LEP and SLC
- Eight pseudo observables describing the physics at the Z-pole are interpreted.



ATLAS Global combination

HIGGS+EW (lin+quad results)

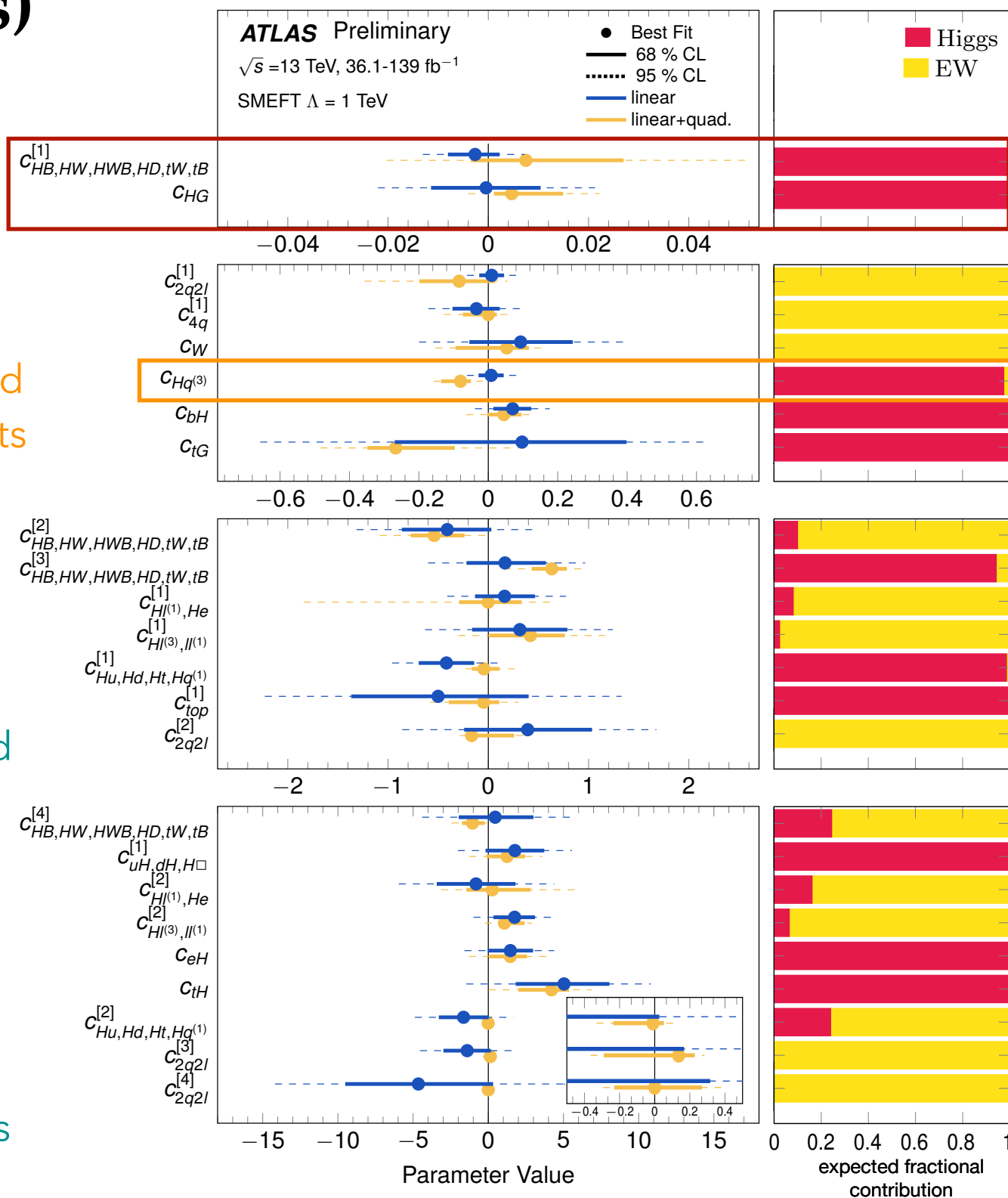
ATL-PHYS-PUB-2022-037

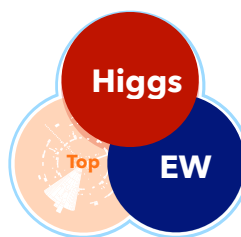
- Principal component analysis to identify sensitive directions-> a modified basis of linear combinations of WCs is defined.
- The fit uses sensitivity eigenvectors instead of original Wilson Coefficient.
- Constraining 7 individual and 17 linear combinations of Wilson coefficients.
- Data overlap across datasets checked -> remove from the combination whenever relevant.

Most stringent constraints

Constrained by both diboson and VH measurements

Weakly constrained fit directions-> quadratic contributions are large; validity of the constraints - neglected higher order contributions

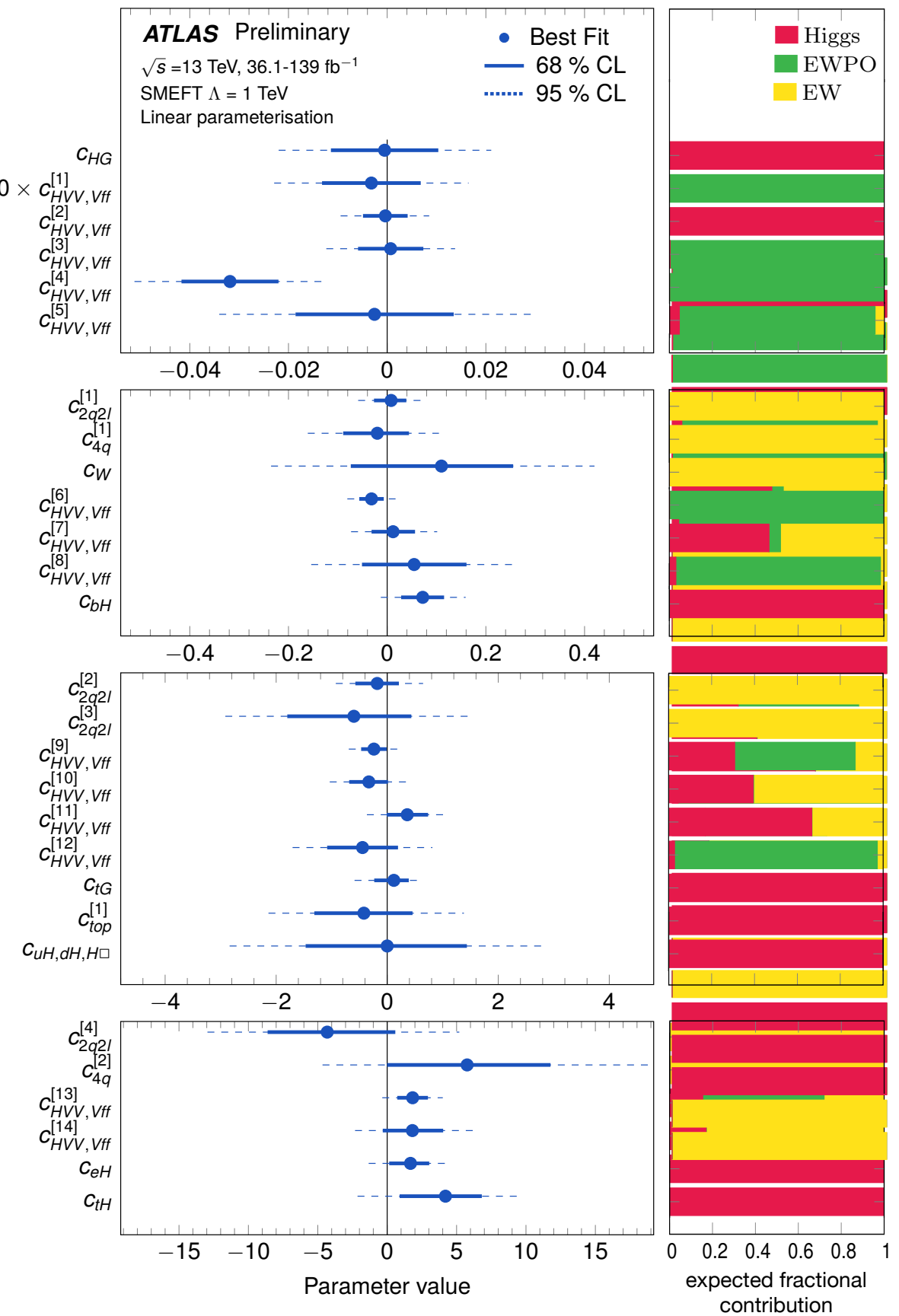




ATLAS Global combination

HIGGS+EW+EWPO

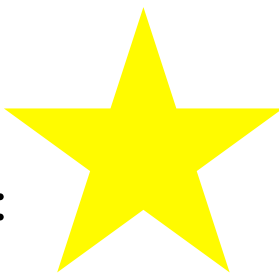
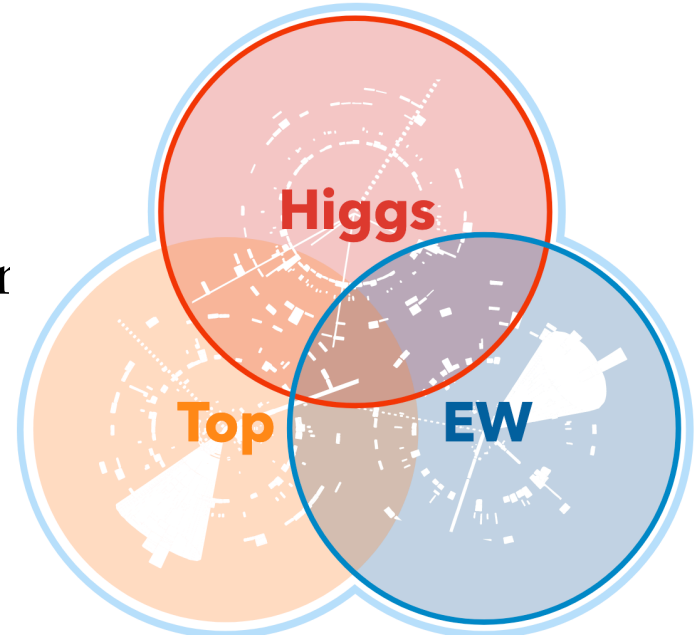
- Constraining 6 individual and 22 linear combinations of Wilson coefficients.
- Several constraints driven by both ATLAS and LEP/SLD.
- Complementary information.
- Linear fits agree with the SM expectation for most fitted parameters, except for:
 - $c_{HVV,Vff}^{[4]}$ → excess driven by a well-known discrepancy in $A_{FB}^{0,b}$ from the SM expectation.



ATL-PHYS-PUB-2022-037

Summary

- Increasing number of analyses in SM, Top and Higgs sectors providing interesting EFT interpretations (additional ATLAS EFT interpretations in Chilufya's, Bo's and Adrian's talks).
- First Global ATLAS EFT interpretation available (also simplified likelihood model for re-interpretation):
 - well established framework used to perform the ATLAS Global combination;
 - combination with additional Top + EW analyses ongoing-> provide complementary sensitivity.
- ATLAS + CMS: ongoing exercise to include few published input measurements and test the combination using consistent parameterisations and assumptions.



for many interesting results to come!!

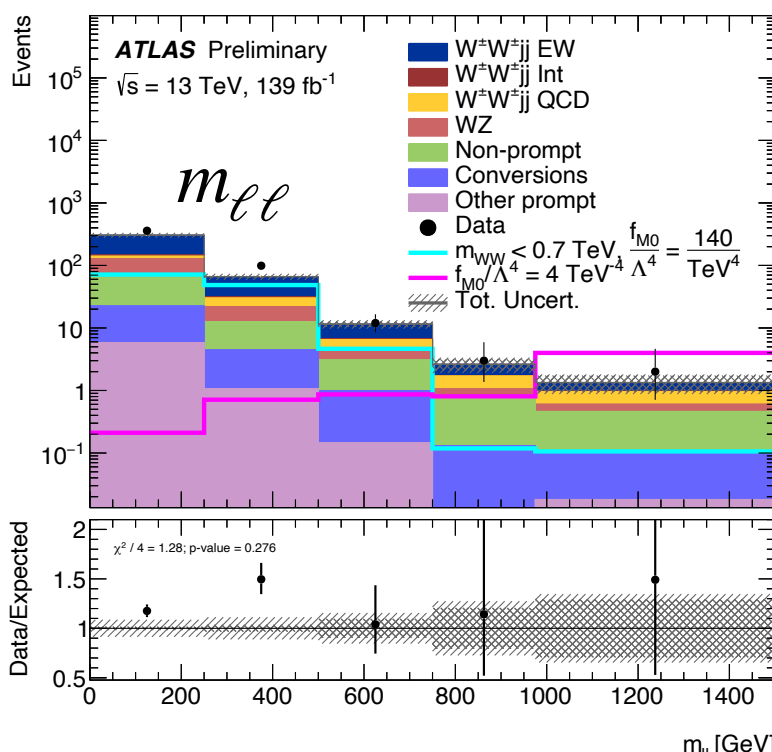
BACKUP



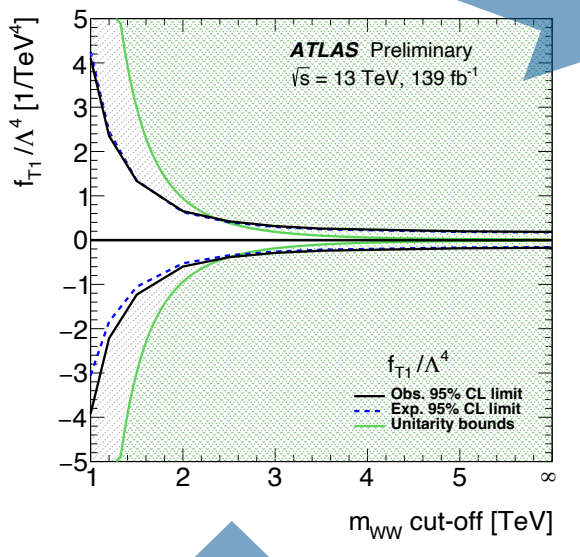
- Fiducial and differential cross sections for the electroweak and inclusive production of a same-sign W boson pair in association with two jets ($W^\pm W^\pm jj$ - (analysis details in Alessandro's talk).
- Differential $m_{\ell\ell}$ distribution with optimised binning used to set limits on EFT dim8 operator coefficients $f_{S02}/\Lambda^4, f_{S1}/\Lambda^4, f_{M0}/\Lambda^4, f_{M1}/\Lambda^4, f_{M7}/\Lambda^4, f_{T0}/\Lambda^4, f_{T1}/\Lambda^4$ and f_{T2}/Λ^4 .
- Results using EFT unitarisation cut-off also provided.
- These constraints are competitive with those previously published by the CMS Collaboration.

Three families of operators (M, S - covariant derivative, T)

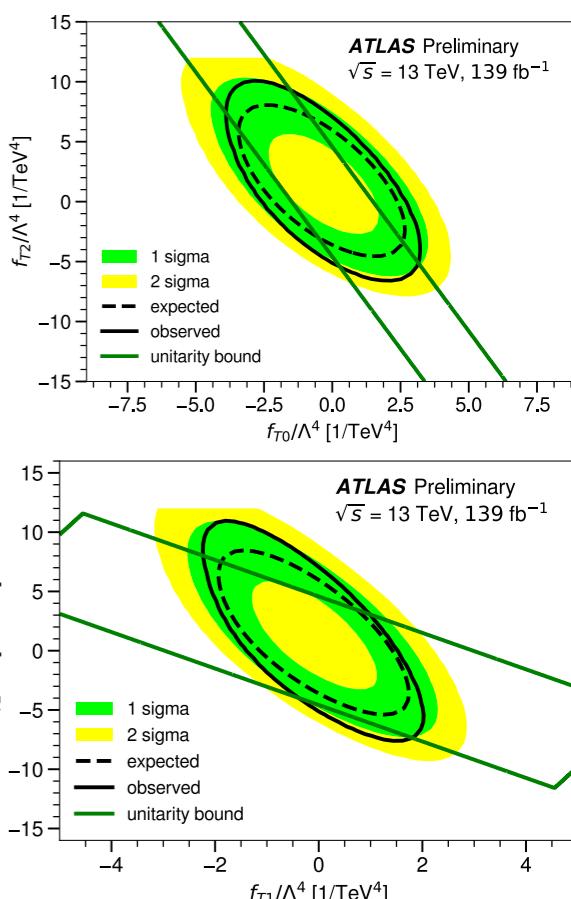
Coefficient	Type	No unitarisation cut-off	Lower and upper limit at the respective unitarity bound
		[TeV $^{-4}$]	[TeV $^{-4}$]
f_{M0}/Λ^4	exp.	[-3.9, 3.8]	-64 at 0.9 TeV, 40 at 1.0 TeV
	obs.	[-4.1, 4.1]	-140 at 0.7 TeV, 117 at 0.8 TeV
f_{M1}/Λ^4	exp.	[-6.3, 6.6]	-25.5 at 1.6 TeV, 31 at 1.5 TeV
	obs.	[-6.8, 7.0]	-45 at 1.4 TeV, 54 at 1.3 TeV
f_{M7}/Λ^4	exp.	[-9.3, 8.8]	-33 at 1.8 TeV, 29.1 at 1.8 TeV
	obs.	[-9.8, 9.5]	-39 at 1.7 TeV, 42 at 1.7 TeV
f_{S02}/Λ^4	exp.	[-5.5, 5.7]	-94 at 0.8 TeV, 122 at 0.7 TeV
	obs.	[-5.9, 5.9]	-
f_{S1}/Λ^4	exp.	[-22.0, 22.5]	-
	obs.	[-23.5, 23.6]	-
f_{T0}/Λ^4	exp.	[-0.34, 0.34]	-3.2 at 1.2 TeV, 4.9 at 1.1 TeV
	obs.	[-0.36, 0.36]	-7.4 at 1.0 TeV, 12.4 at 0.9 TeV
f_{T1}/Λ^4	exp.	[-0.158, 0.174]	-0.32 at 2.6 TeV, 0.44 at 2.4 TeV
	obs.	[-0.174, 0.186]	-0.38 at 2.5 TeV, 0.49 at 2.4 TeV
f_{T2}/Λ^4	exp.	[-0.56, 0.70]	-2.60 at 1.7 TeV, 10.3 at 1.2 TeV
	obs.	[-0.63, 0.74]	-

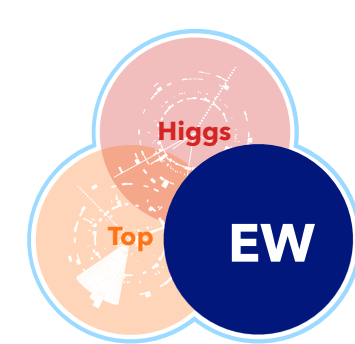


2D limits at 95% CL obtained with a unitarisation cut-off scale of 1.5 TeV



Evolution of the limits as a function of the cut-off scale of the unitarisation procedure.



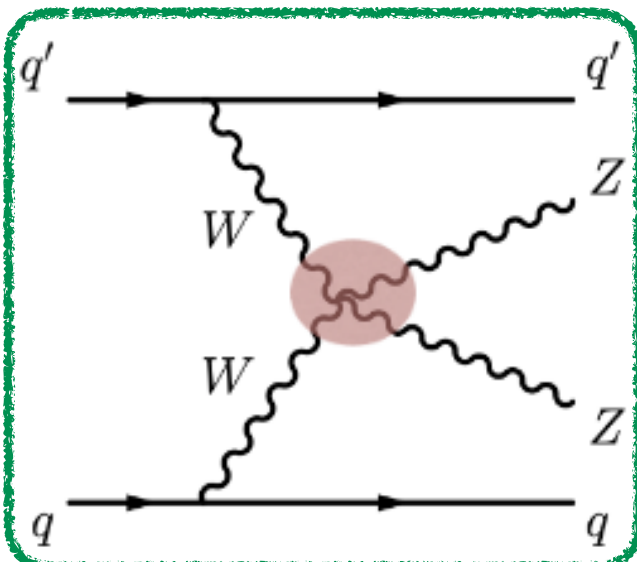


41 VBS measurements

ATLAS-CONF-2023-024

- Differential cross-sections ($m_{4\ell}$ and m_{jj}) measured for the production of four charged leptons in association with two jets (analysis details in Chilufya's talk).
- Unfolded cross sections used to search for signatures of anomalous weak-boson self-interactions using the framework of dim6 and dim8 EFT.

$$\mathcal{O}_{T0}, \mathcal{O}_{T1}, \mathcal{O}_{T2}, \mathcal{O}_{T5}, \mathcal{O}_{T6}, \mathcal{O}_{T7}, \mathcal{O}_{T8}, \mathcal{O}_{T9}$$

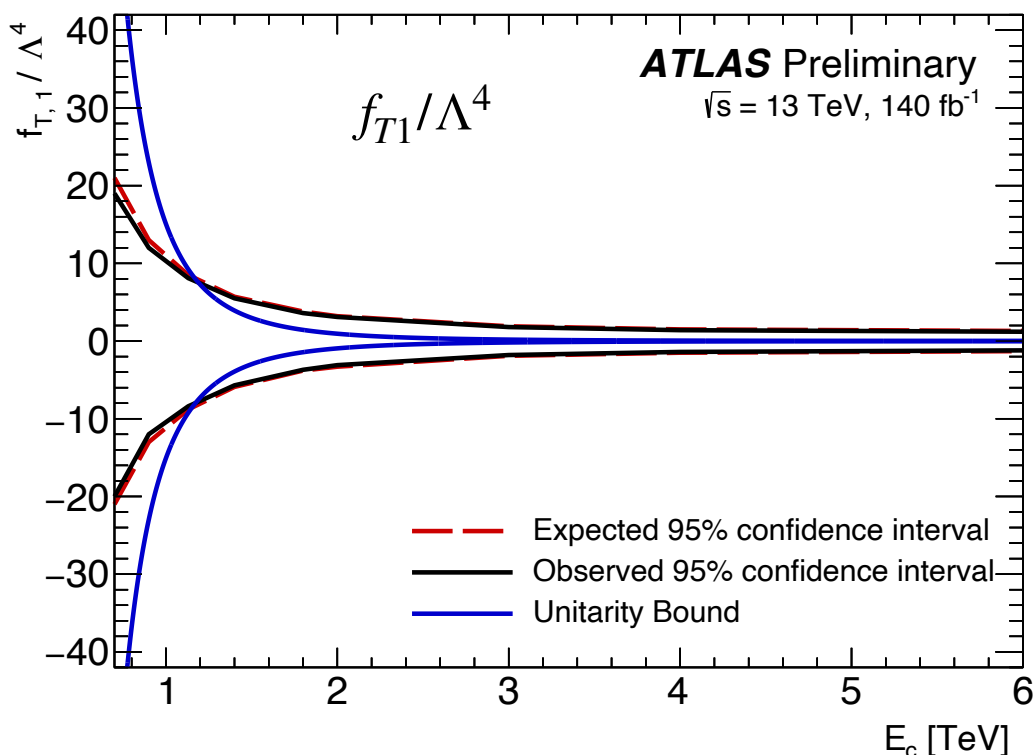


- The WCs associated with the \mathcal{O}_{T0} and \mathcal{O}_{T1} operators are the most tightly constrained.
- Constraints with the pure dim8 contribution are more stringent than interference-only constraints

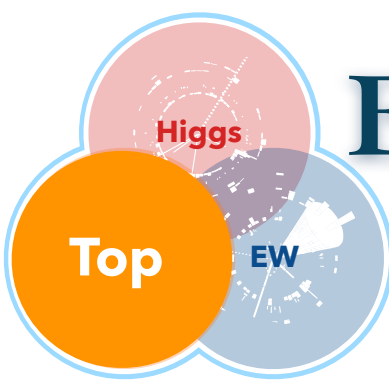
field strength
tensors

Wilson coefficient	$ \mathcal{M}_{d8} ^2$	95% confidence interval [TeV $^{-4}$]	
	Included	Expected	Observed
$f_{T,0}/\Lambda^4$	yes	[-0.98, 0.93]	[-1.0, 0.97]
	no	[-23, 17]	[-19, 19]
$f_{T,1}/\Lambda^4$	yes	[-1.2, 1.2]	[-1.3, 1.3]
	no	[-160, 120]	[-140, 140]
$f_{T,2}/\Lambda^4$	yes	[-2.5, 2.4]	[-2.6, 2.5]
	no	[-74, 56]	[-63, 62]
$f_{T,5}/\Lambda^4$	yes	[-2.5, 2.4]	[-2.6, 2.5]
	no	[-79, 60]	[-68, 67]
$f_{T,6}/\Lambda^4$	yes	[-3.9, 3.9]	[-4.1, 4.1]
	no	[-64, 48]	[-55, 54]
$f_{T,7}/\Lambda^4$	yes	[-8.5, 8.1]	[-8.8, 8.4]
	no	[-260, 200]	[-220, 220]
$f_{T,8}/\Lambda^4$	yes	[-2.1, 2.1]	[-2.2, 2.2]
	no	$[-4.6, 3.1] \times 10^4$	$[-3.9, 3.8] \times 10^4$
$f_{T,9}/\Lambda^4$	yes	[-4.5, 4.5]	[-4.7, 4.7]
	no	$[-7.5, 5.5] \times 10^4$	$[-6.4, 6.3] \times 10^4$

- Constraints are placed on each WC after restricting the interference- and pure dimension-eight contributions to have $m_{4\ell} < E_c$
- The 95% confidence intervals degrade by a factor of 4-5 when the energy scale cut off is reduced from $E_c = \infty$ to $E_c = 1$ TeV.

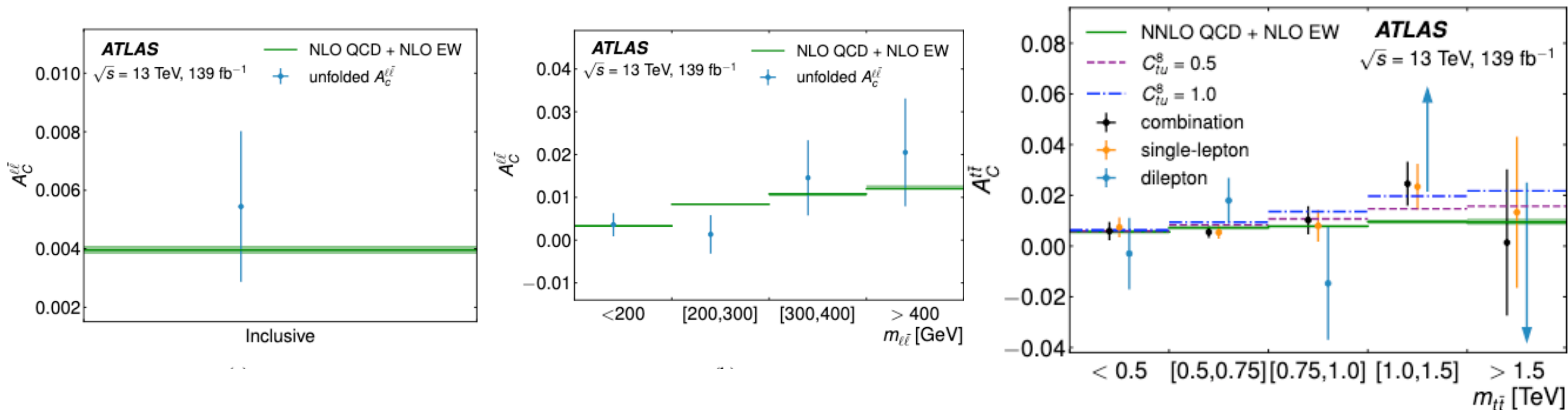


Evidence for the charge asymmetry in $pp \rightarrow t\bar{t}$



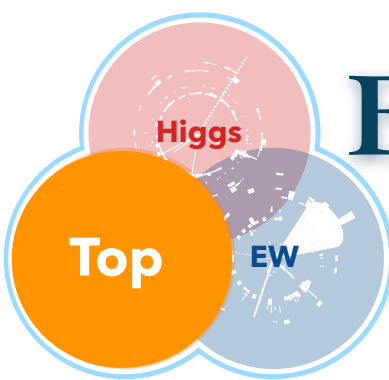
[arxiv:2208.12095](https://arxiv.org/abs/2208.12095)

- Inclusive and differential full Run2 measurements of the top–antitop ($t\bar{t}$) charge asymmetry $A_c^{t\bar{t}}$ and the leptonic asymmetry $A_c^{\ell\bar{\ell}}$
- Differential measurements are performed as a function of the invariant mass, transverse momentum and longitudinal boost of the $t\bar{t}$ system.
- Combined results are interpreted in the SMEFT framework.
- **14 four-fermion operators** + 1 operator for top–gluon interaction.



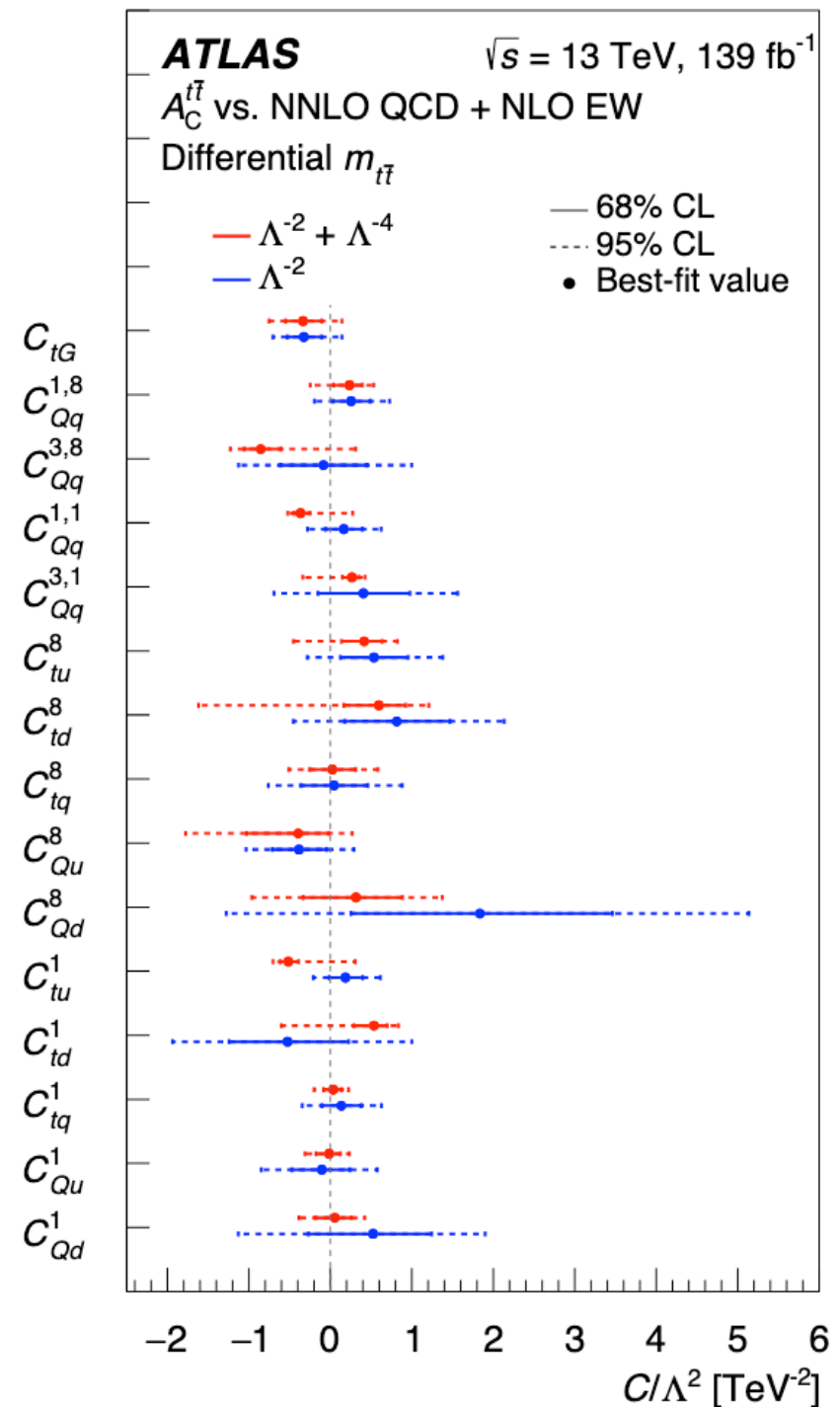
The combined inclusive charge asymmetry is measured to be $A_c^{t\bar{t}} = 0.0068 \pm 0.0015$, which differs from zero by **4.7 standard deviations**.

Evidence for the charge asymmetry in $pp \rightarrow t\bar{t}$

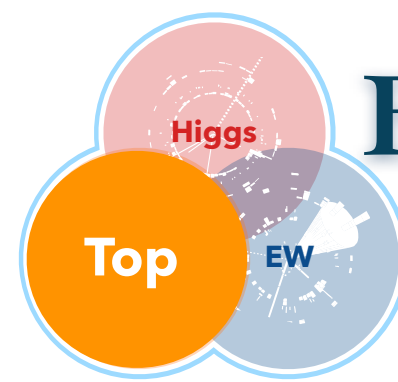


[arxiv:2208.12095](https://arxiv.org/abs/2208.12095)

- Inclusive and differential full Run2 (139 fb^{-1}) measurements of $t\bar{t}$ and leptonic charge asymmetry $A_c^{t\bar{t}}$ & $A_c^{\ell\bar{\ell}}$.
- Differential measurements provided for invariant mass, transverse momentum and longitudinal boost of the $t\bar{t}$ system.
- Combined results are interpreted in the **SMEFT** framework.
- **14 four-fermion operators** + 1 operator for top–gluon interaction.
- Large improvement w.r.t LHC 8TeV / Tevatron results.
- Interplay between sensitivity (increases for higher $m_{t\bar{t}}$) and uncertainty (0.2% – 0.3% to 2.9%).
- Tightest linear limit obtained in the mass bin from 1 to 1.5 TeV.
- Constraint from the differential $m_{t\bar{t}}$ measurement more than a factor 2 stronger than inclusive measurement.



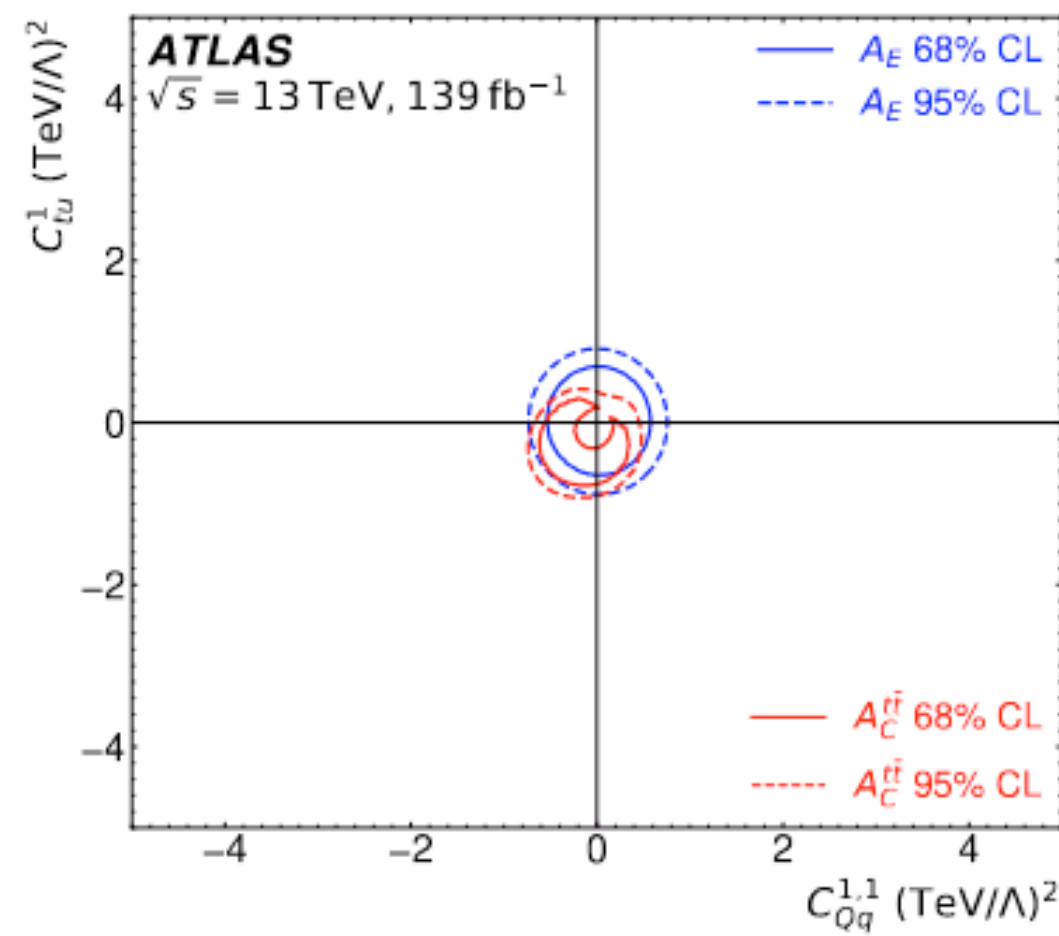
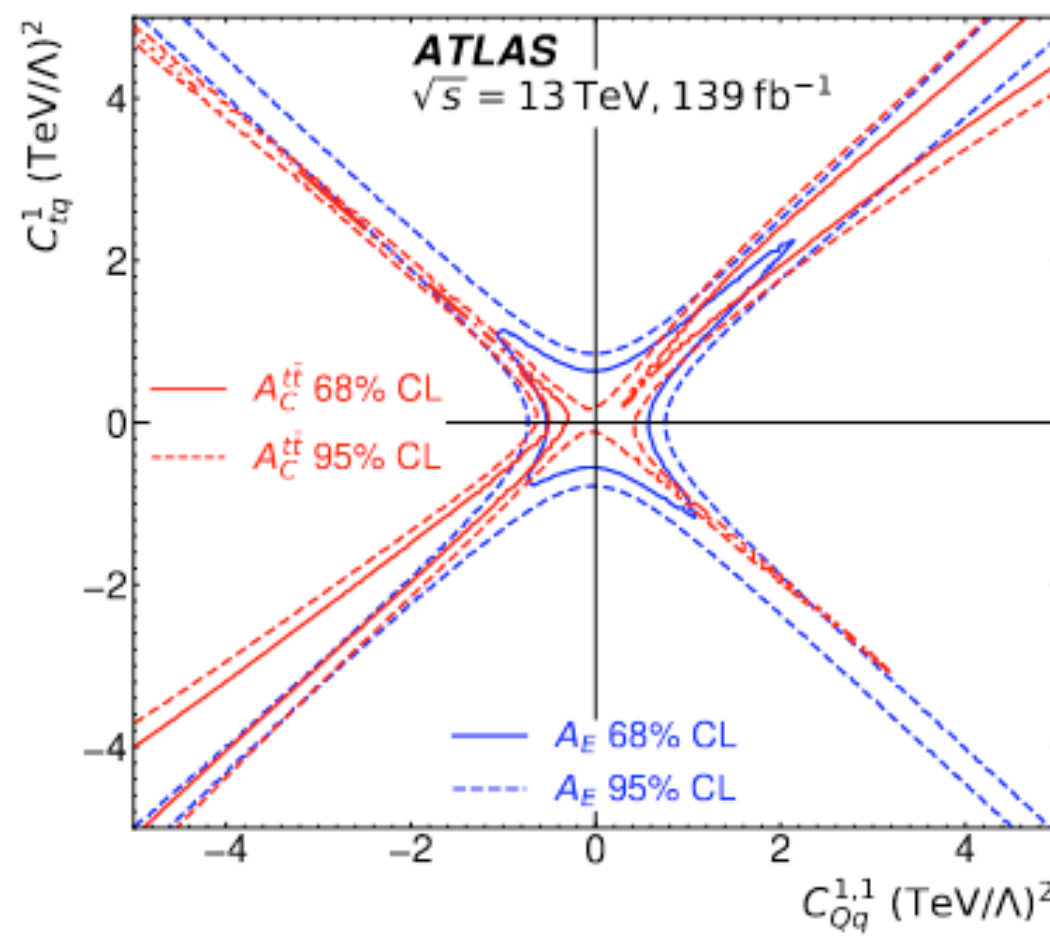
The combined inclusive charge asymmetry is measured to be $A_c^{t\bar{t}} = 0.0068 \pm 0.0015$, which differs from zero by 4.7 standard deviations.



Evidence for the charge asymmetry in $pp \rightarrow t\bar{t}$

[arxiv:2208.12095](https://arxiv.org/abs/2208.12095)

- QCD structure of the energy asymmetry not the same as for the charge asymmetry in $t\bar{t}$ production due to the extra jet in $t\bar{t}j$ production.
 - the two asymmetries probe different directions in chiral and colour space.
- For colour-singlet operators with different quark chiralities (top row), the two asymmetries probe similar areas in the parameter space.



Evidence for the charge asymmetry in $pp \rightarrow t\bar{t}$

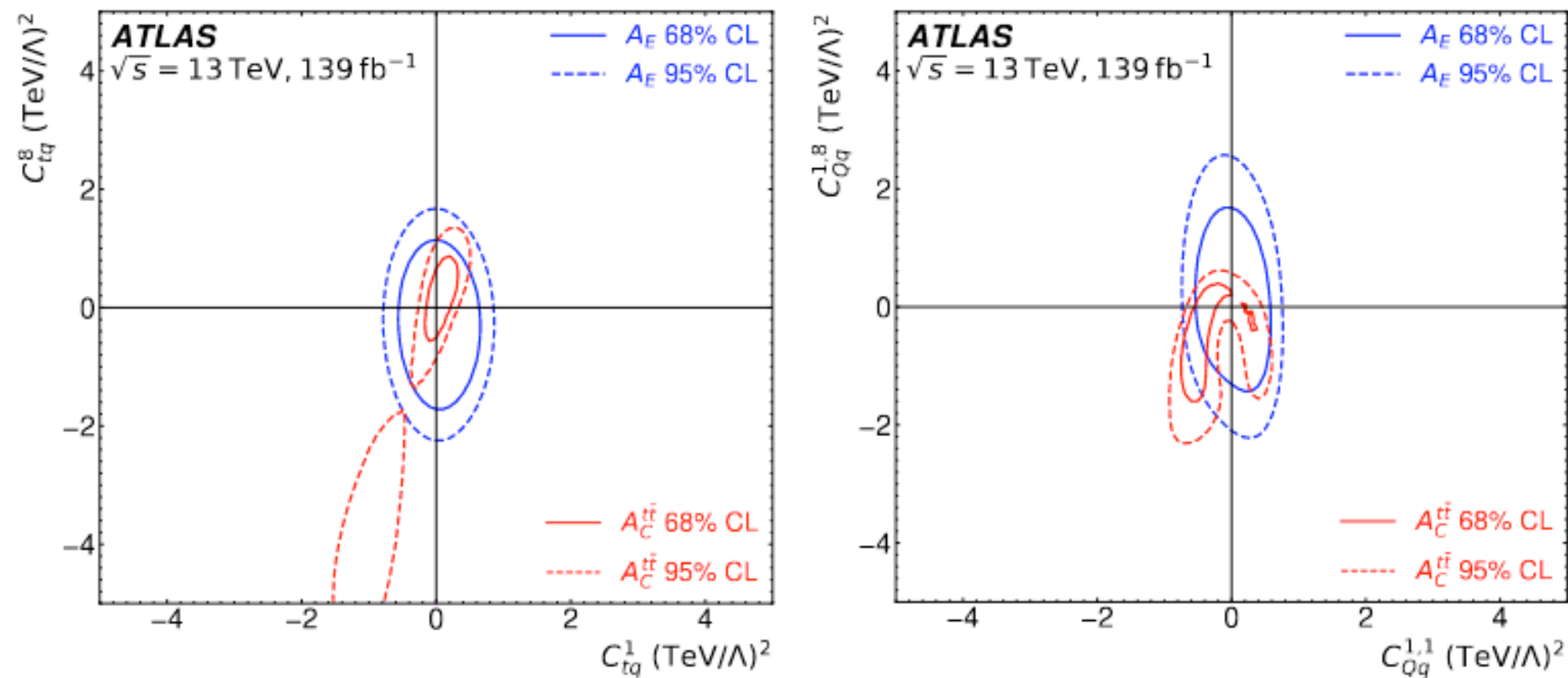
Higgs

Top

EW

[arxiv:2208.12095](https://arxiv.org/abs/2208.12095)

- QCD structure of the energy asymmetry not the same as for the charge asymmetry in $t\bar{t}$ production due to the extra jet in $t\bar{t}j$ production.
 - the two asymmetries probe different directions in chiral and colour space.
- Different shapes of the bounds are due to the different colour-singlet and colour-octet contributions to $t\bar{t}$ and $t\bar{t}j$ production, which is probed with high sensitivity by the asymmetries.

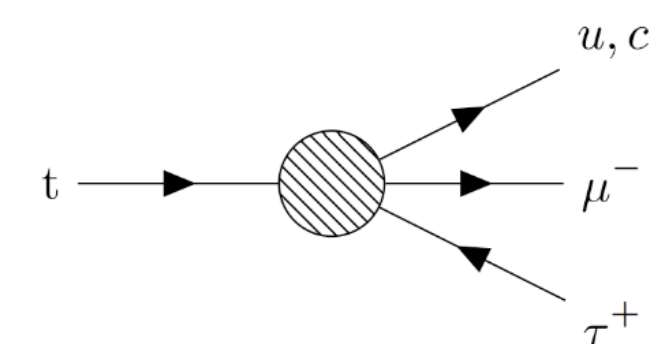
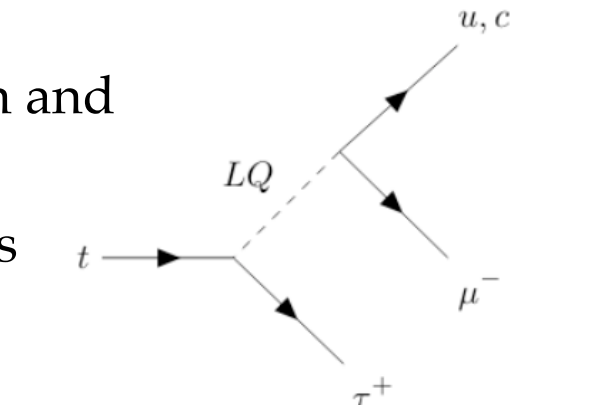


colour-singlet versus colour-octet operators with the same quark chiralities

Search for charged lepton flavour violation in top quark decays

[ATLAS-CONF-2023-001](#)

- Search for charged-lepton-flavour violating $\mu\tau qt$ interaction in top-quark production and decay.
- The analysis sensitivity is dominated by the cLFV production process; decay process improves the observed limits by 2.7%
- EFT interpretation: dedicated samples to set limits on EFT operators describing contact interactions between two leptons and two quarks permitting cLFV interactions (dim6-top).
- Cross section of the cLFV process: dependence on the square of the value of WC.



	95% CL upper limits on Wilson coefficients $c/\Lambda^2 [\text{TeV}^{-2}]$							
	$c_{lq}^{-(ijk3)}$	$c_{eq}^{(ijk3)}$	$c_{lu}^{(ijk3)}$	$c_{eu}^{(ijk3)}$	$c_{lequ}^{1(ijk3)}$	$c_{lequ}^{1(ij3k)}$	$c_{lequ}^{3(ijk3)}$	$c_{lequ}^{3(ij3k)}$
Previous (u) [22]	12	12	12	12	26	26	3.4	3.4
Expected (u)	0.47	0.44	0.43	0.46	0.49	0.49	0.11	0.11
Observed (u)	0.49	0.47	0.46	0.48	0.51	0.51	0.11	0.11
Previous (c) [22]	14	14	14	14	29	29	3.7	3.7
Expected (c)	1.6	1.6	1.5	1.6	1.8	1.8	0.35	0.35
Observed (c)	1.7	1.6	1.6	1.6	1.9	1.9	0.37	0.37

	95% CL upper limits on BR($t \rightarrow \mu\tau q$)	
	Stat. only	All systematics
Expected	8×10^{-7}	10×10^{-7}
Observed	9×10^{-7}	11×10^{-7}

Statistically dominated, dominant sys: $t\bar{t}$ modelling

- The limits obtained on the Wilson coefficients improve upon the previous results from a re-interpretation of an ATLAS FCNC tZq analysis (from a factor of 8 to 51) - [JHEP 04 \(2019\) 014](#).
- This result complements searches for cLFV in $e\mu qt$ interactions by the CMS Collaboration. [JHEP 06 \(2022\) 082](#) [CMS-PAS-TOP-22-005](#)

Search for charged lepton flavour violation in top quark decays

[ATLAS-CONF-2023-001](#)

- EFT interpretation: use dedicated samples to set limits on EFT operators describing contact interactions between two leptons and two quarks permitting cLFV interactions (dim6top model).
- The cross section of the cLFV process depends on the square of the value of the relevant Wilson coefficient for a given value of the scale of new physics.

	95% CL upper limits on $\text{BR}(t \rightarrow \mu\tau q) \times 10^{-7}$							
	$c_{lq}^{-(ijk3)}$	$c_{eq}^{(ijk3)}$	$c_{lu}^{(ijk3)}$	$c_{eu}^{(ijk3)}$	$c_{lequ}^{1(ijk3)}$	$c_{lequ}^{1(ij3k)}$	$c_{lequ}^{3(jik3)}$	$c_{lequ}^{3(ij3k)}$
Expected (u)	4.6	4.2	4.0	4.5	2.5	2.5	5.8	5.8
Observed (u)	5.1	4.6	4.4	5.0	2.8	2.8	6.4	6.4
Expected (c)	54	51	51	52	35	35	61	61
Observed (c)	60	56	56	57	38	38	68	68

Operator	Lorentz Structure	
$O_{lq}^{1(ijkl)}$	$(\bar{l}_i \gamma^\mu l_j)(\bar{q}_k \gamma_\mu q_l)$	Vector
$O_{lq}^{3(ijkl)}$	$(\bar{l}_i \gamma^\mu \sigma^I l_j)(\bar{q}_k \gamma_\mu \sigma^I q_l)$	Vector
$O_{eq}^{(ijkl)}$	$(\bar{e}_i \gamma^\mu e_j)(\bar{q}_k \gamma_\mu q_l)$	Vector
$O_{lu}^{(ijkl)}$	$(\bar{l}_i \gamma^\mu l_j)(\bar{u}_k \gamma_\mu u_l)$	Vector
$O_{eu}^{(ijkl)}$	$(\bar{e}_i \gamma^\mu e_j)(\bar{u}_k \gamma_\mu u_l)$	Vector
$\pm O_{lequ}^{1(ijkl)}$	$(\bar{l}_i e_j) \epsilon(\bar{q}_k u_l)$	Scalar
$\pm O_{lequ}^{3(ijkl)}$	$(\bar{l}_i \sigma^{\mu\nu} e_j) \epsilon(\bar{q}_k \sigma_{\mu\nu} u_l)$	Tensor

top-quark decay width Γ

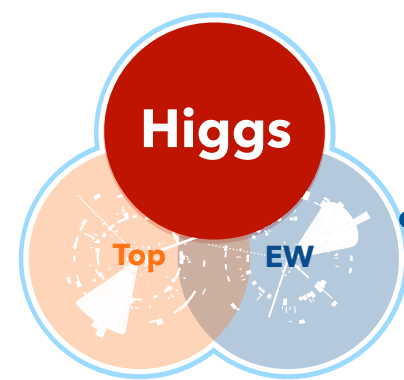
$$\begin{aligned} \Gamma(t \rightarrow \ell_i^+ \ell_j^- q_k) = & \frac{m_t}{6144\pi^3} \left(\frac{m_t}{\Lambda} \right)^4 \left\{ 4|c_{lq}^{-(ijk3)}|^2 + 4|c_{eq}^{(ijk3)}|^2 + 4|c_{lu}^{(ijk3)}|^2 + 4|c_{eu}^{(ijk3)}|^2 \right. \\ & \left. + |c_{lequ}^{1(jik3)}|^2 + |c_{lequ}^{1(ij3k)}|^2 + 48|c_{lequ}^{3(jik3)}|^2 + 48|c_{lequ}^{3(ij3k)}|^2 \right\} \end{aligned}$$

VBF HWW

Higgs

Top

EW



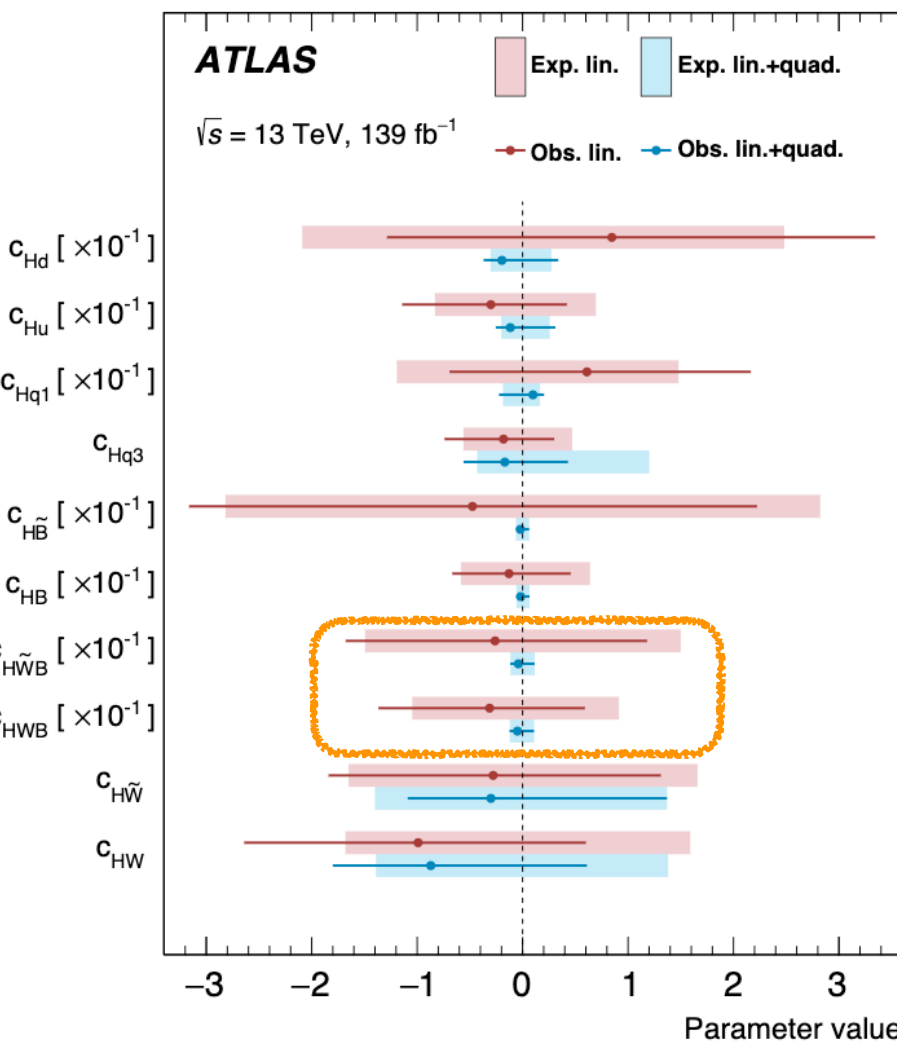
- Integrated and differential fiducial (first in VBF) cross-section measurements for VBF in the HWW $e\nu\mu\nu$ channel.

- Differential cross-sections used to constrain extensions to the SM using an EFT approach:

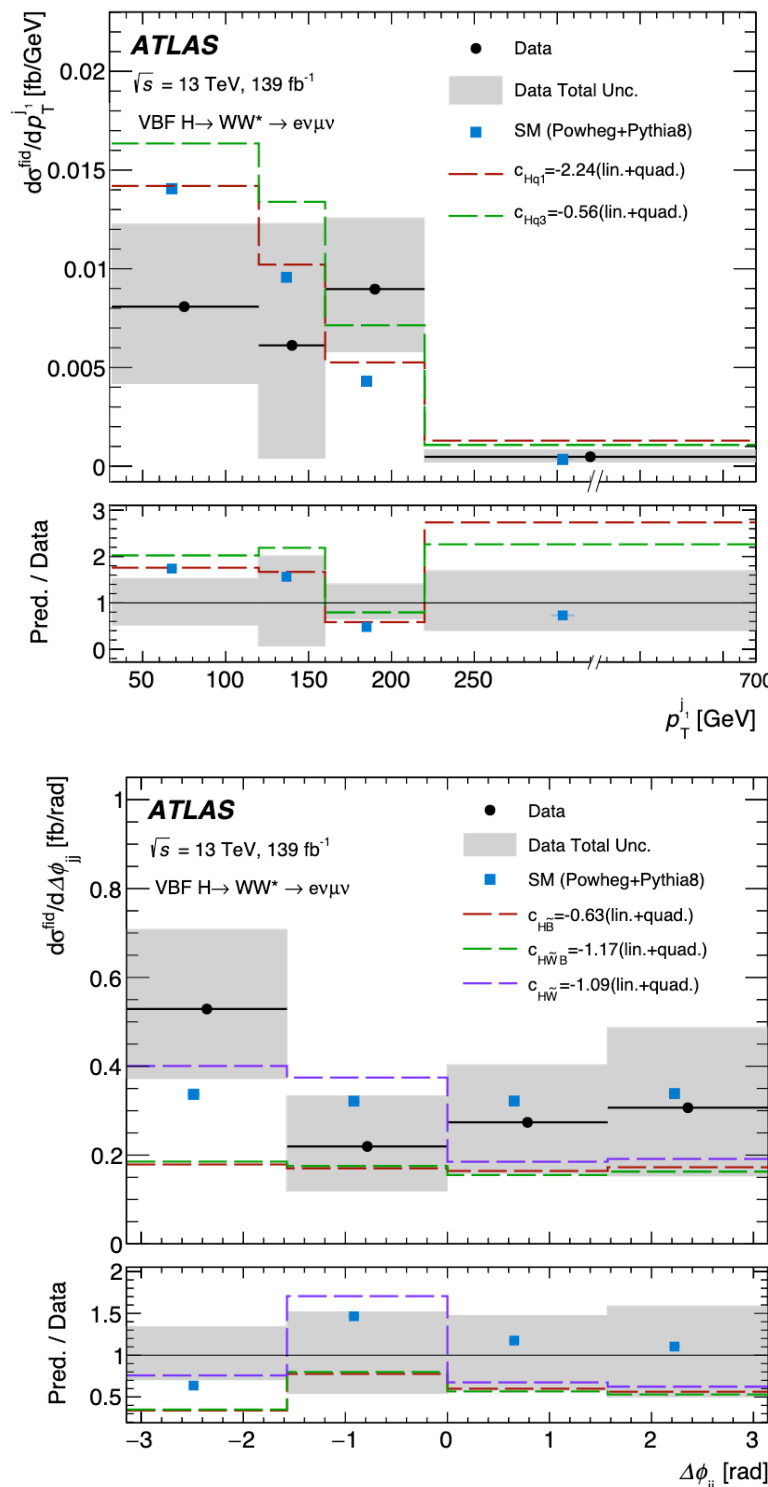
$$\mathcal{L}_{\text{EFT}} = \mathcal{L}_{\text{SM}} + \sum_d \sum_i \frac{c_i^{(d)}}{\Lambda^{(d-4)}} O_i^{(d)}, \text{ for } d > 4.$$

SMEFTsim

- The WCs are constrained one at a time using the differential distribution that is most sensitive to the corresponding operator ($\Delta\phi_{jj}$ - CP-odd, leading jet pT - CP-even)



- More stringent constraints for all WCs when the quadratic term is added to the parameterization.
- Neglected contributions of higher-dimensional operators in the EFT expansion.
- Correlations obtained between central values of EFT operators using the bootstrapping technique.
(backup)



Higgs**Top****EW**

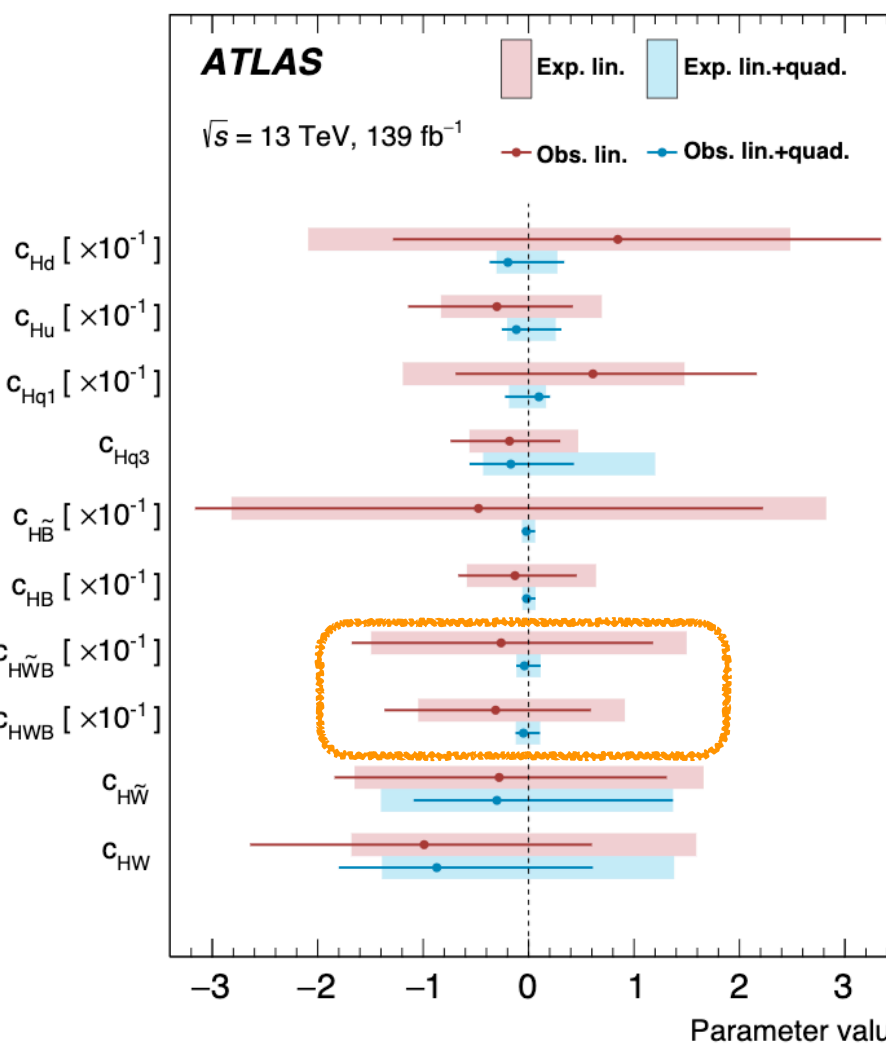
VBF HWW

- Integrated and differential fiducial (first in VBF) cross-section measurements for VBF in the HWW $e\nu\mu\nu$ channel (139 fb^{-1}).
- Differential cross-sections used to constrain extensions to the SM using an EFT approach:

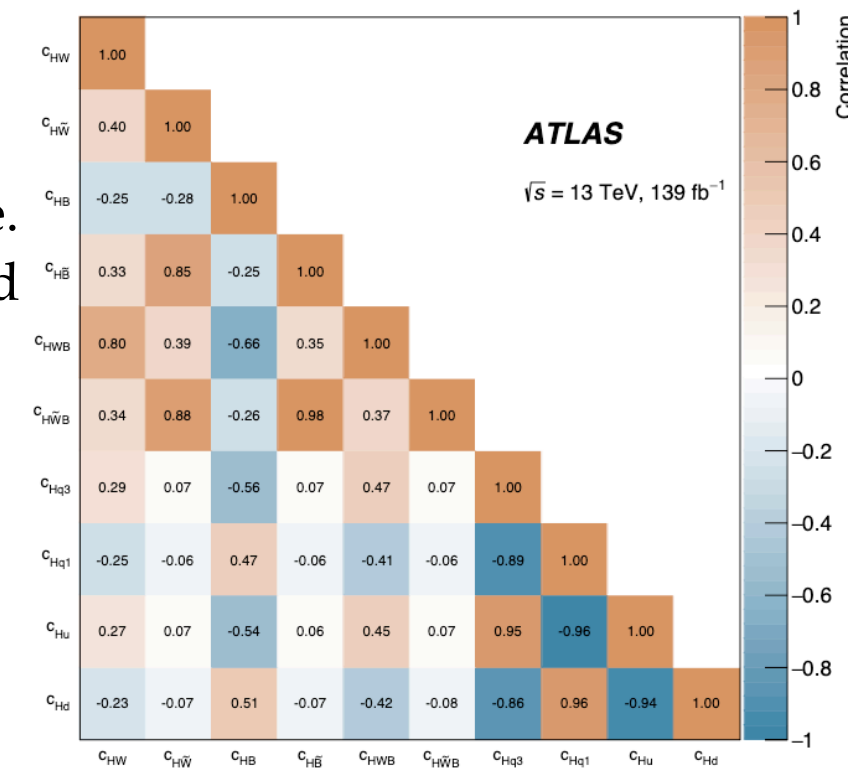
$$\mathcal{L}_{\text{EFT}} = \mathcal{L}_{\text{SM}} + \sum_d \sum_i \frac{c_i^{(d)}}{\Lambda^{(d-4)}} O_i^{(d)}, \text{ for } d > 4.$$

SMEFTsim

- The WCs are constrained one at a time using the differential distribution that is most sensitive to the corresponding operator ($\Delta\phi_{jj}$ - CP-odd, leading jet pT - CP-even)



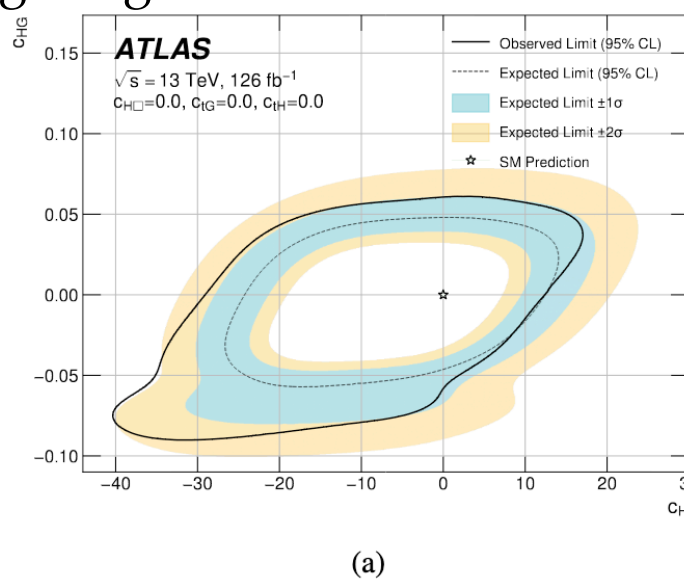
- Correlations obtained between central values of EFT operators using the bootstrapping technique.
- Pairs of measurements can be used to set constraints on new and different models of physics beyond the SM, for example in future global fits



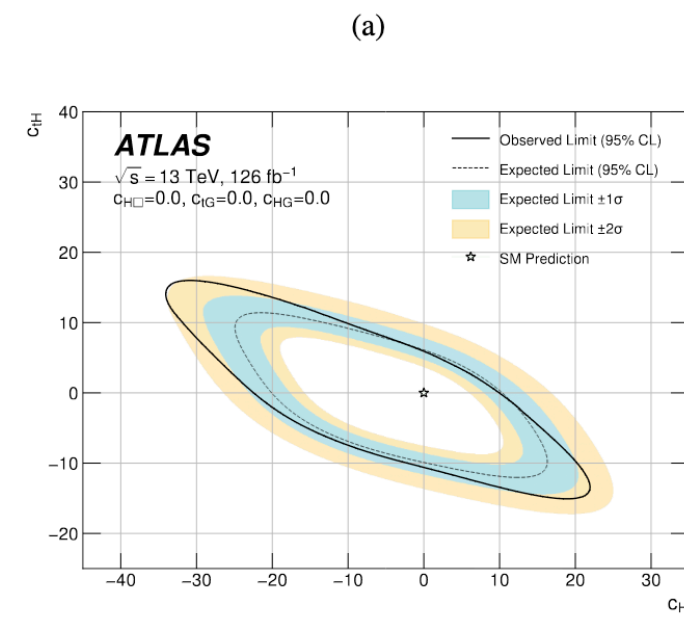
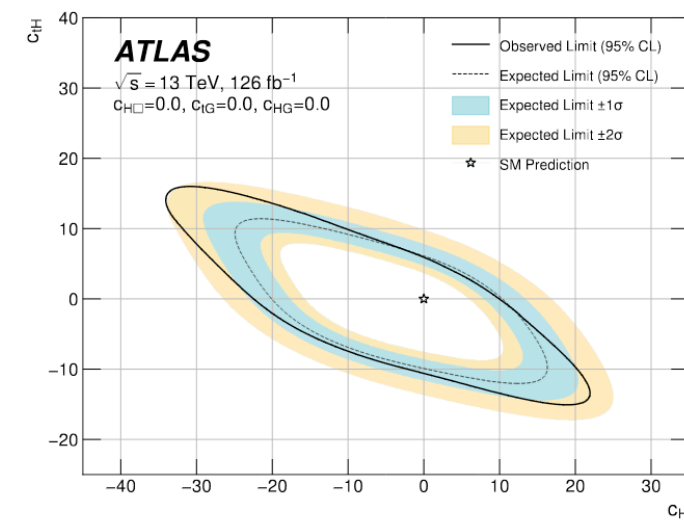
HH(4b) SMEFT

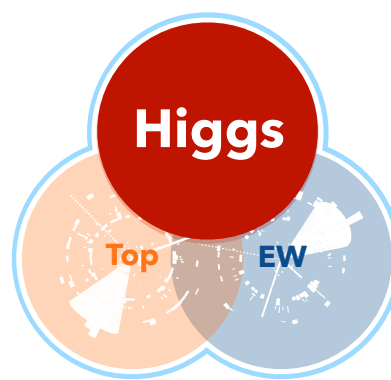
- Non-resonant HH production ggF production mode - 4b decay channel (126 fb^{-1}).
- Analysis categorisations to improve sensitivity to BSM physics.
- The interpretations are performed with two EFT frameworks, Higgs Effective Field Theory (HEFT) and SM Effective Field Theory (SMEFT).
 - first LHC SMEFT interpretation for HH.
- The different BSM scenarios are considered re-weighting the SM non-resonant HH ggF sample.
- 1D and 2D limits for the 5 Wilson coefficients: $c_H, c_{H\square}, c_{tH}, c_{tG}, c_{HG}$. SMEFT@NLO

Parameter	Expected Constraint		Observed Constraint	
	Lower	Upper	Lower	Upper
c_H	-20	11	-22	11
c_{HG}	-0.056	0.049	-0.067	0.060
$c_{H\square}$	-9.3	13.9	-8.9	14.5
c_{tH}	-10.0	6.4	-10.7	6.2
c_{tG}	-0.97	0.94	-1.12	1.15

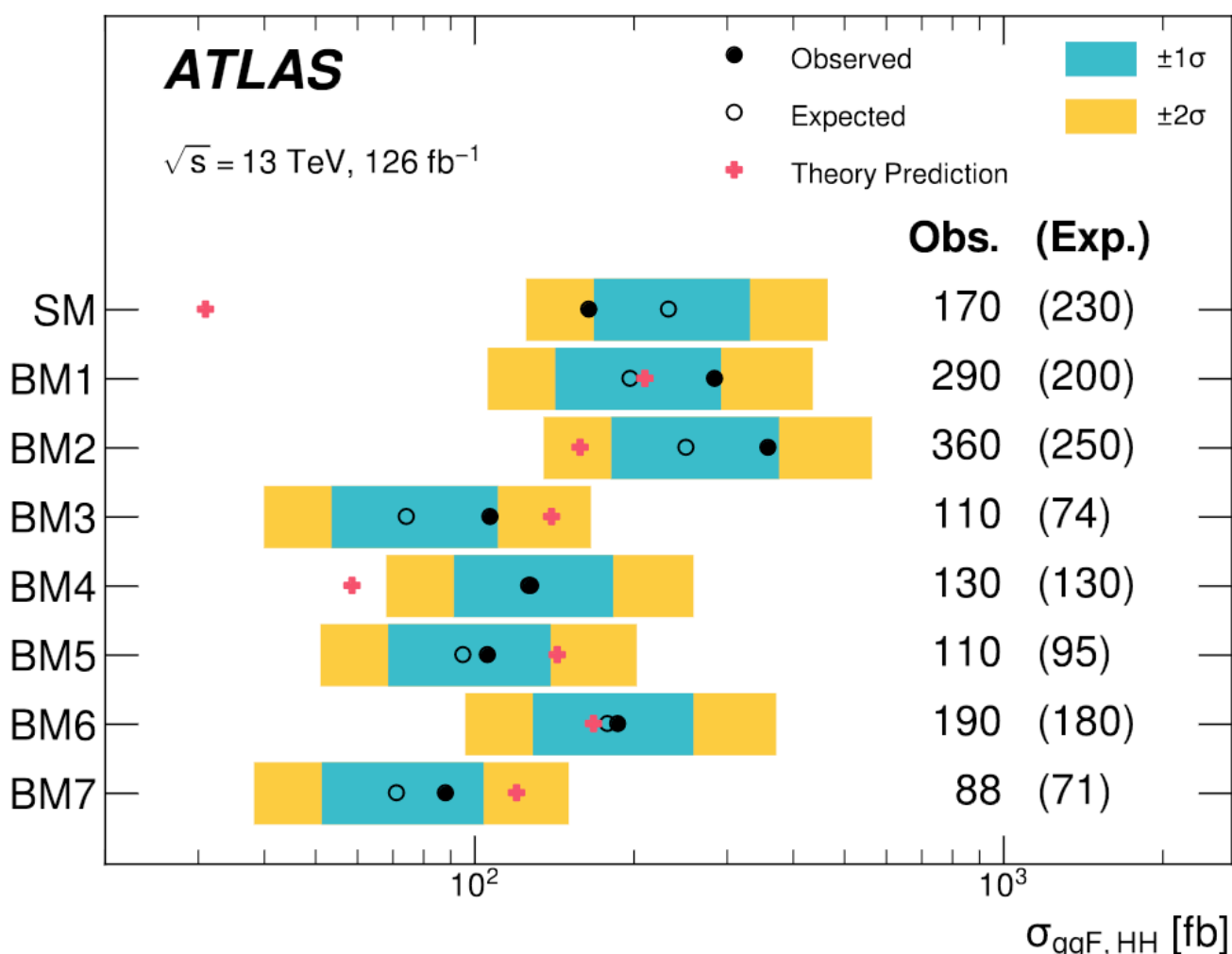


(a)





- 7 HEFT benchmark models for $c_{HHH}, c_{ttH}, c_{ttHH}, c_{ggH}$ and c_{ggHH} to probe a wide variety of characteristic shapes of the m_{HH} spectrum.
- Advantage of HEFT: anomalous single-Higgs-boson and HH couplings defined separately.
- The spread of sensitivity between the seven benchmark models reflects the different shapes of the signal m_{HH} distributions.



The different variation between observed and expected limits is linked to a slight excess observed in the low m_{HH} region

- Limits competitive with ATLAS $b\bar{b}\tau\tau + b\bar{b}\gamma\gamma$ standalone limits -> improvement when included in the combination

$HH \rightarrow 4b$

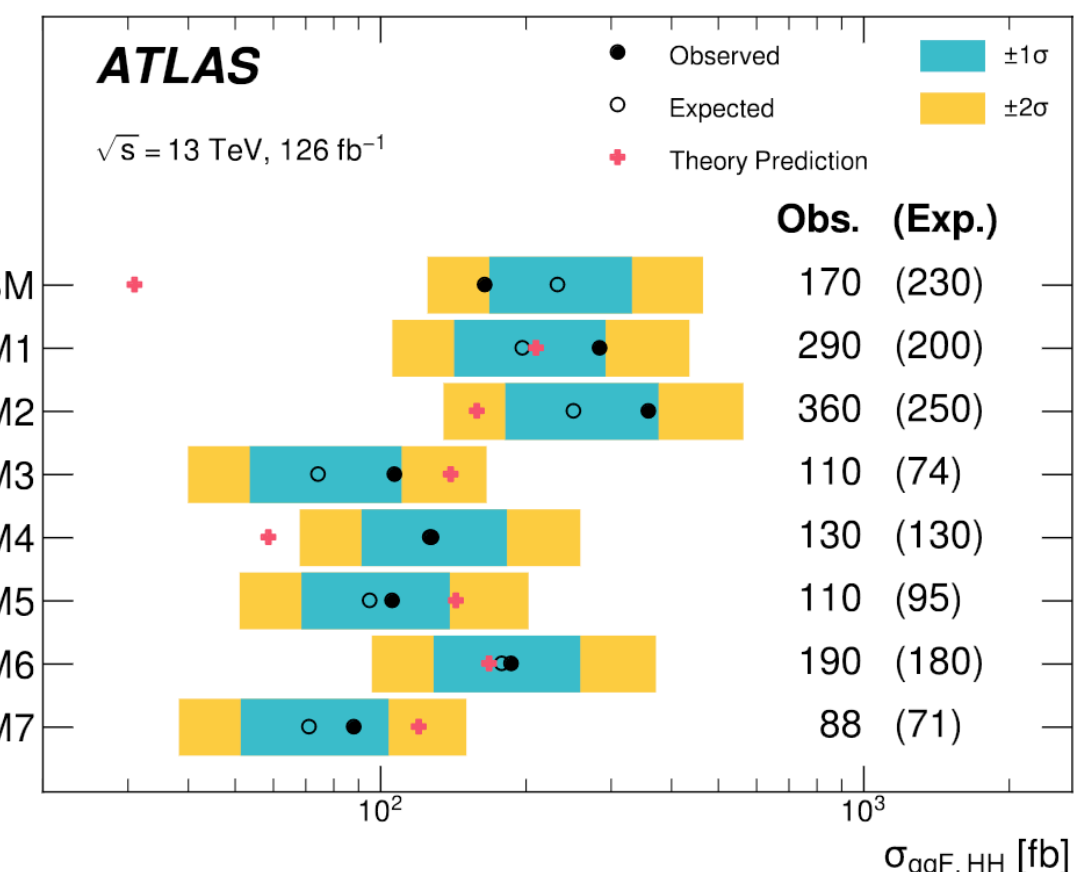
c_{gghh}	[-0.36,0.78] [-0.42,0.75]				
$c_{t\bar{t}HH}$	[-0.55,0.51] [-0.46,0.40]				
$HH \rightarrow b\bar{b}\gamma\gamma$		$HH \rightarrow b\bar{b}\tau\tau$	$b\bar{b}\tau\tau + b\bar{b}\gamma\gamma$		
Wilson coefficient	Obs.	Exp.	Obs.	Exp.	Combination
c_{gghh}	[-0.4, 0.5]	[-0.5, 0.7]	[-0.4, 0.4]	[-0.4, 0.4]	[-0.3, 0.4]
$c_{t\bar{t}HH}$	[-0.3, 0.8]	[-0.4, 0.9]	[-0.3, 0.7]	[-0.2, 0.6]	[-0.2, 0.6]

[ATL-PHYS-PUB-2022-019](https://cds.cern.ch/record/2914231)



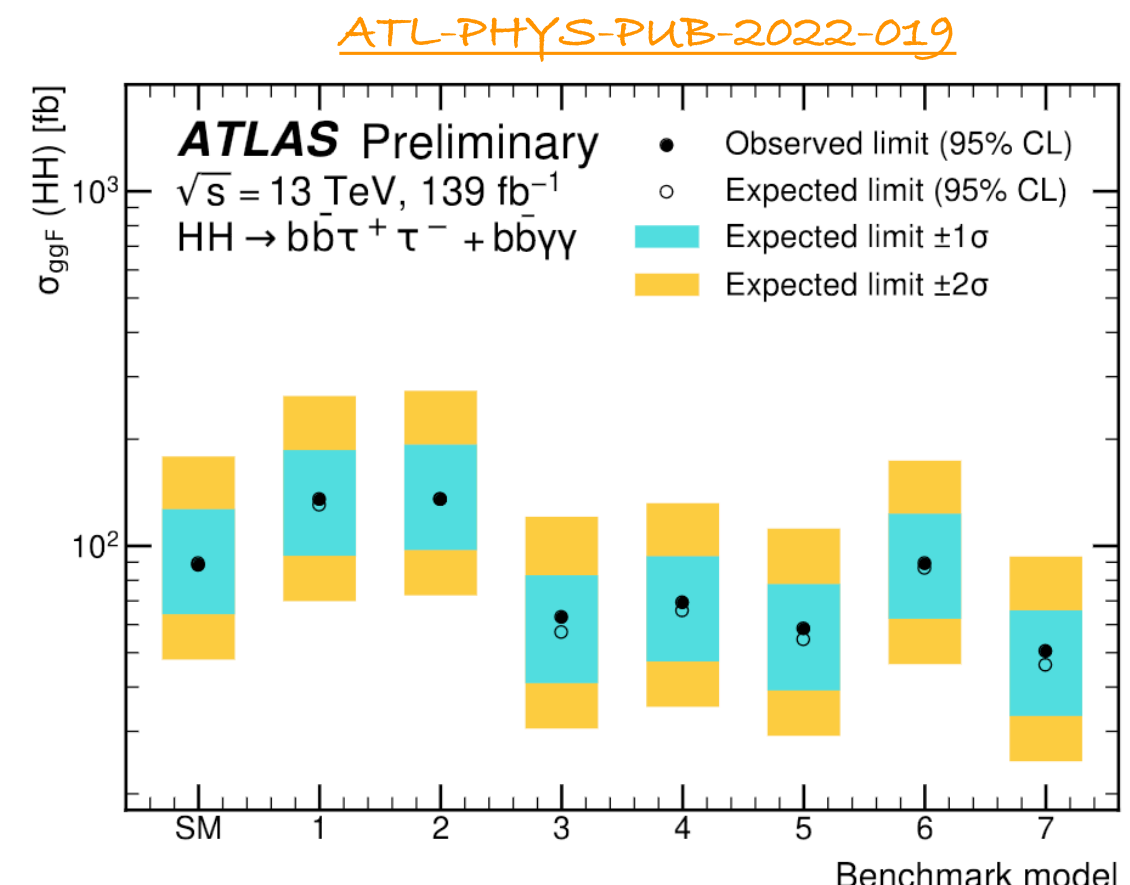
- 7 HEFT benchmark models for $c_{HHH}, c_{ttH}, c_{ttHH}, c_{ggH}$ and c_{ggHH} to probe a wide variety of characteristic shapes of the m_{HH} spectrum.
- Advantage of HEFT: anomalous single-Higgs-boson and HH couplings defined separately.
- The spread of sensitivity between the seven benchmark models reflects the different shapes of the signal m_{HH} distributions.

Benchmark Model	c_{HHH}	c_{ttH}	c_{ggH}	c_{ggHH}	c_{ttHH}
SM	1	1	0	0	0
BM1	3.94	0.94	1/2	1/3	-1/3
BM2	6.84	0.61	0.0	-1/3	1/3
BM3	2.21	1.05	1/2	1/2	-1/3
BM4	2.79	0.61	-1/2	1/6	1/3
BM5	3.95	1.17	1/6	-1/2	-1/3
BM6	5.68	0.83	-1/2	1/3	1/3
BM7	-0.10	0.94	1/6	-1/6	1

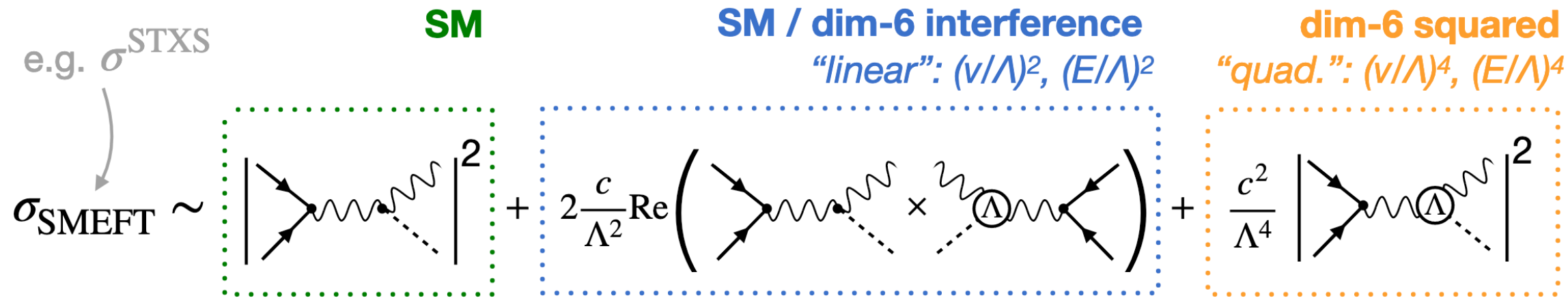


The different variation between observed and expected limits is linked to a slight excess observed in the low m_{HH} region

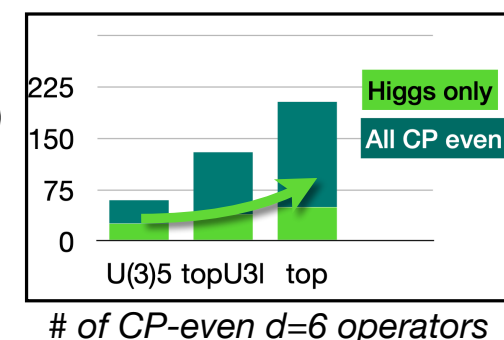
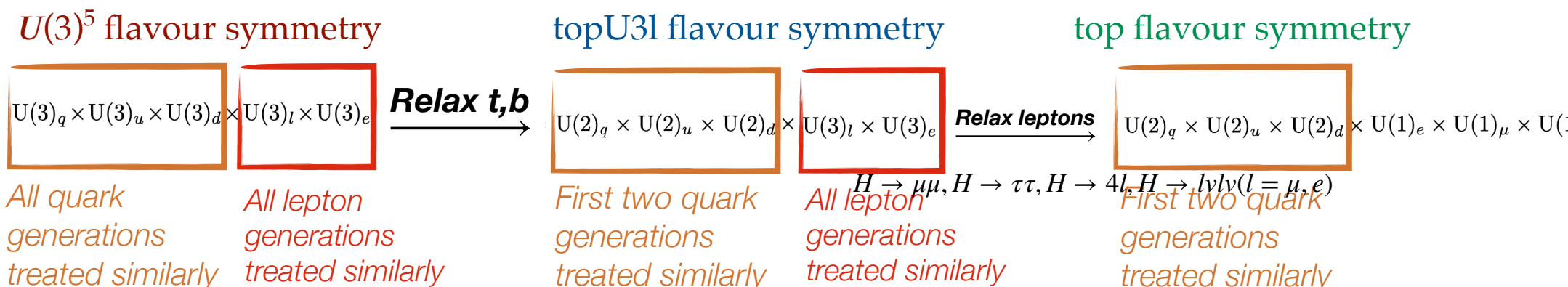
- Limits competitive with $b\bar{b}\tau\tau + b\bar{b}\gamma\gamma$ standalone limits
-> improvement when included in the combination

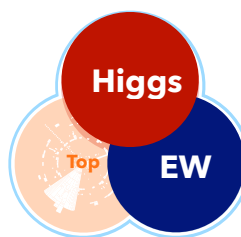


Global combination: SMEFT parameterisation



- Warsaw basis, assuming $\Lambda = 1 \text{ TeV}$.
- SMEFTsim + SMEFT@NLO + TopFCNC.
- Results are usually provided for **linear** model (+ **linear-quadratic** models).
- SMEFTsim: different flavour symmetries used to reduce the number of Wilson coefficients.
("U(3)⁵ flavour symmetry", "topU3I")



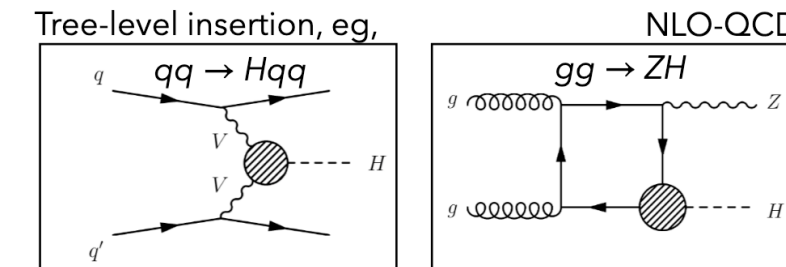


Global combination: SMEFT parameterisation



The impact of dim-6 CP-even operators is estimated using both MC truth and analytical predictions for all the Wilson coefficients that have numerically relevant contributions (62).

- Dimension-six operator effects are calculated:
 - at tree level using SMEFTsim 3.0.
 - for processes that are loop-induced in the SM, thus ggH and $ggZH$ production, Higgs boson decays into gluons -> SMEFTatNLO.
 - Analytic formulas for $H \rightarrow \gamma\gamma$ including NLO EW corrections and LEP observables.
- Theory uncertainties on SM predictions, no additional uncertainties on SMEFT.
- Acceptance corrections to account for kinematic differences between SM and SMEFT in Higgs boson decays on both **linear** and **linear+quadratic** terms.
- Effects of width changes of intermediate particles (“propagator corrections”) included.



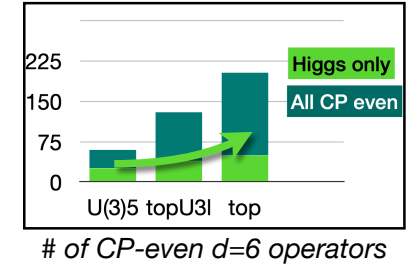
SMEFT sim v3.0 **SMEFT@NLO**

First ATLAS Global combination

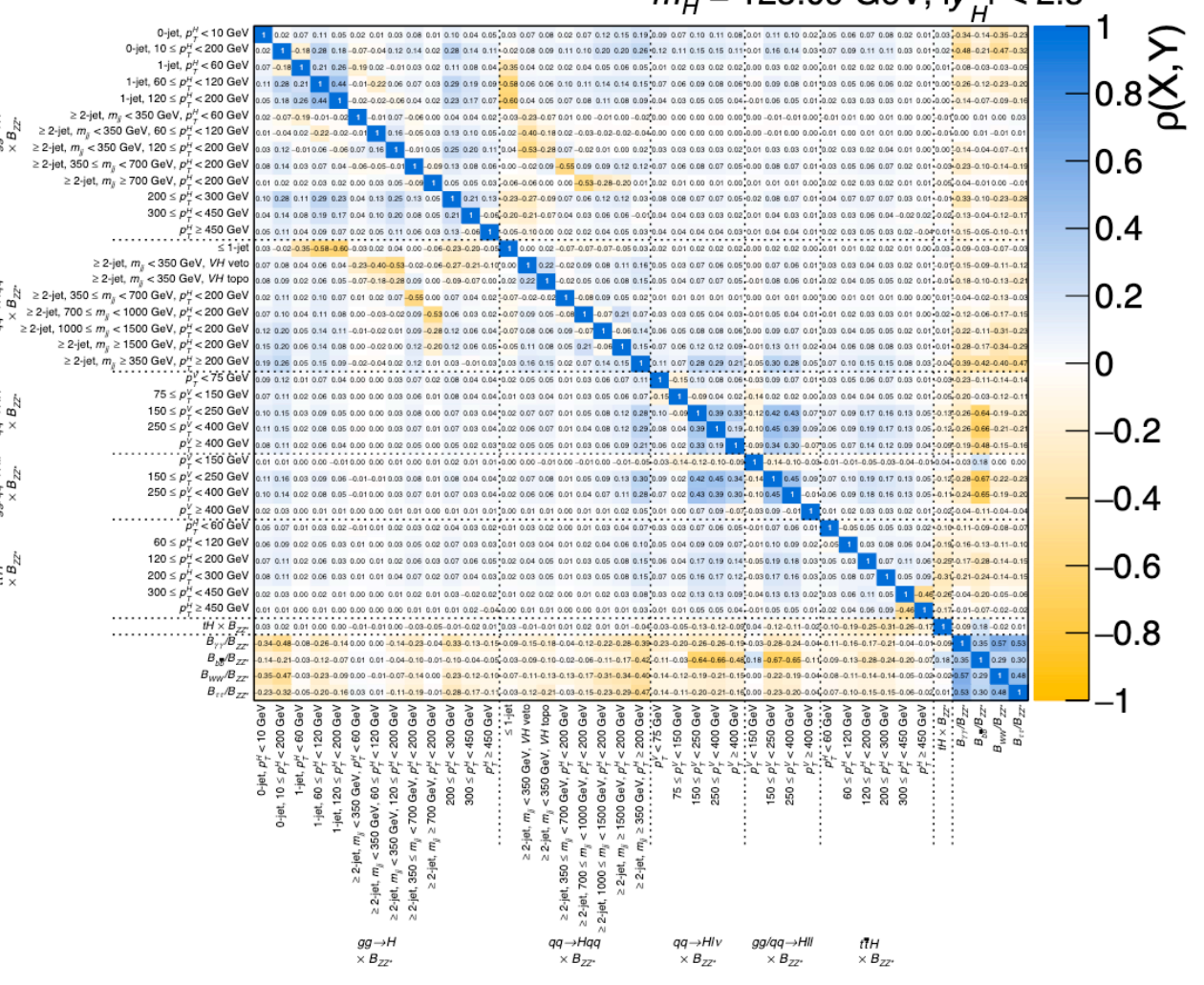
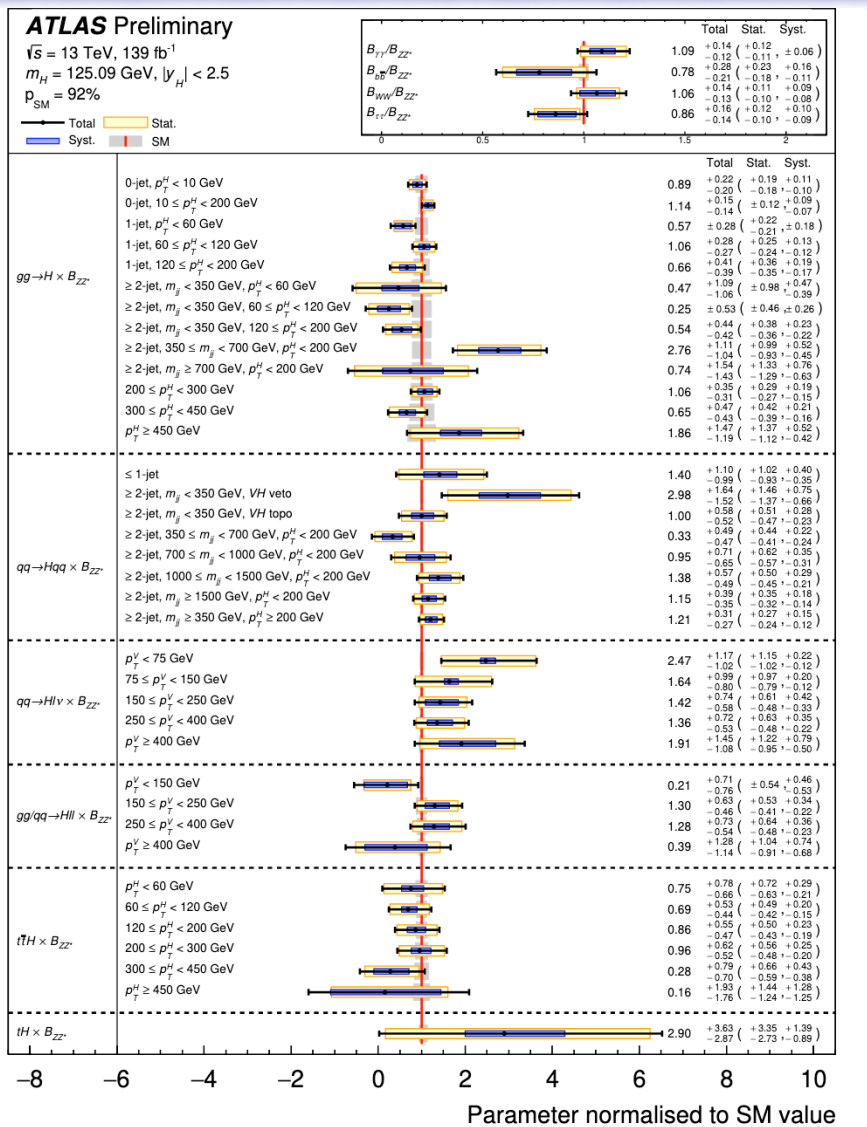
Higgs Combination

Decay channel	Target Production Modes	$\mathcal{L} [\text{fb}^{-1}]$
$H \rightarrow \gamma\gamma$	ggF, VBF, WH, ZH, $t\bar{t}H$, tH	139
$H \rightarrow ZZ^*$	ggF, VBF, WH, ZH, $t\bar{t}H(4\ell)$	139
$H \rightarrow WW^*$	ggF, VBF	139
$H \rightarrow \tau\tau$	ggF, VBF, WH, ZH, $t\bar{t}H(\tau_{\text{had}}\tau_{\text{had}})$	139
	WH, ZH	139
$H \rightarrow b\bar{b}$	VBF	126
	$t\bar{t}H$	139

- ATLAS Higgs boson data (2021 combination)
- Higgs boson production and decay combined measurements in STXS bins



SMEFTsim: “topU31” flavour symmetry”



First ATLAS Global combination

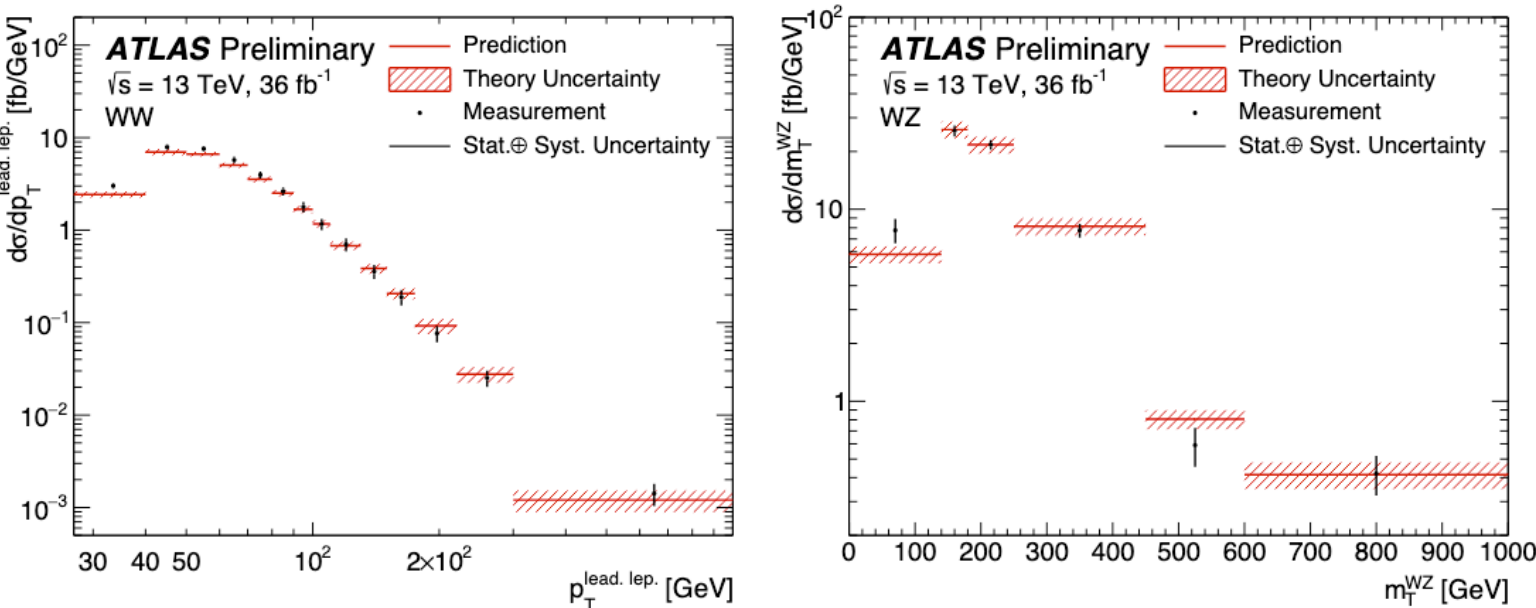
WW,WZ,4l, Z+2jets combination

$$L(\mathbf{x}|\mathbf{c}, \boldsymbol{\theta}) = \frac{1}{\sqrt{(2\pi)^{n_{\text{bins}}} \det(V)}} \exp\left(-\frac{1}{2}\Delta\mathbf{x}^\top(\mathbf{c}, \boldsymbol{\theta})V^{-1}\Delta\mathbf{x}(\mathbf{c}, \boldsymbol{\theta})\right)$$

$$\times \prod_i^{n_{\text{theo syst}}} f_i(\theta_{\text{theo syst},i}) \times \prod_i^{n_{\text{exp syst}}} f_i(\theta_{\text{exp syst},i}).$$

$$\Delta x_b(\mathbf{c}, \boldsymbol{\theta}) = x_b^{\text{meas}}(\boldsymbol{\theta}) - x_b^{\text{pred}}(\mathbf{c}, \boldsymbol{\theta}).$$

Multivariate gaussian

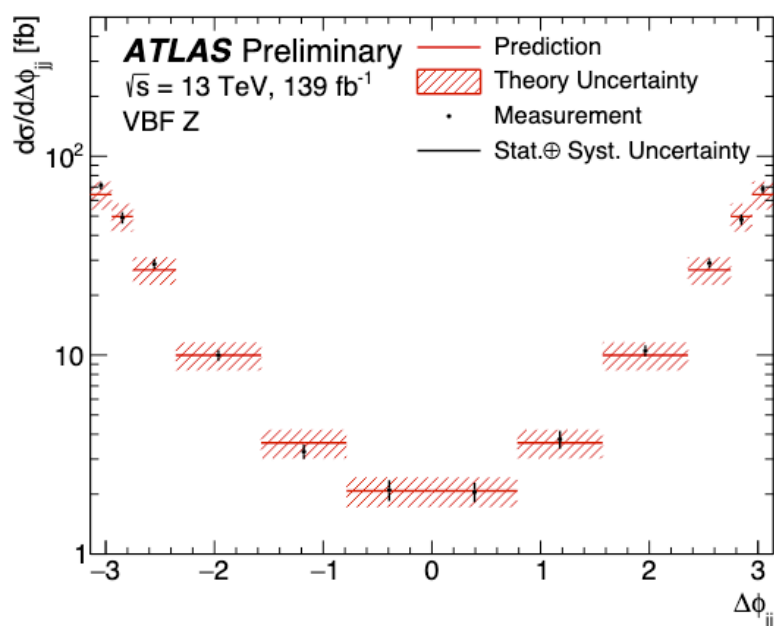
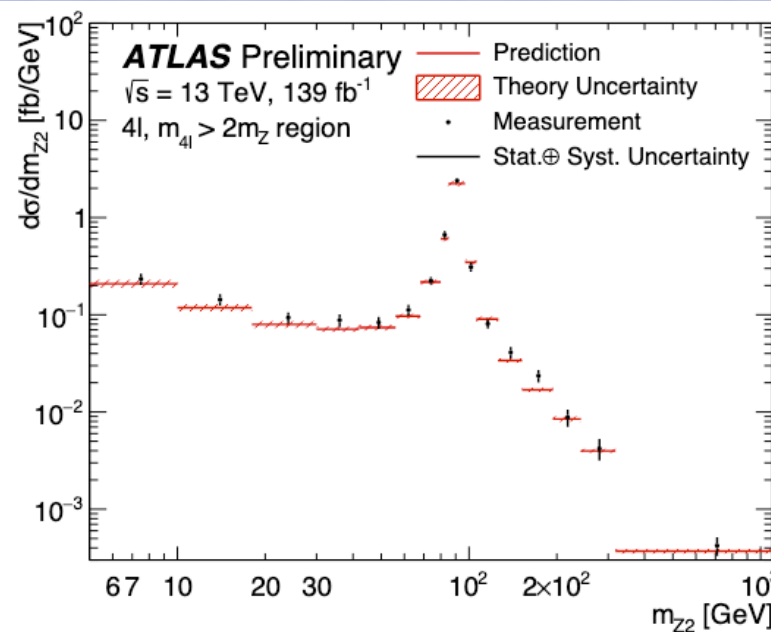
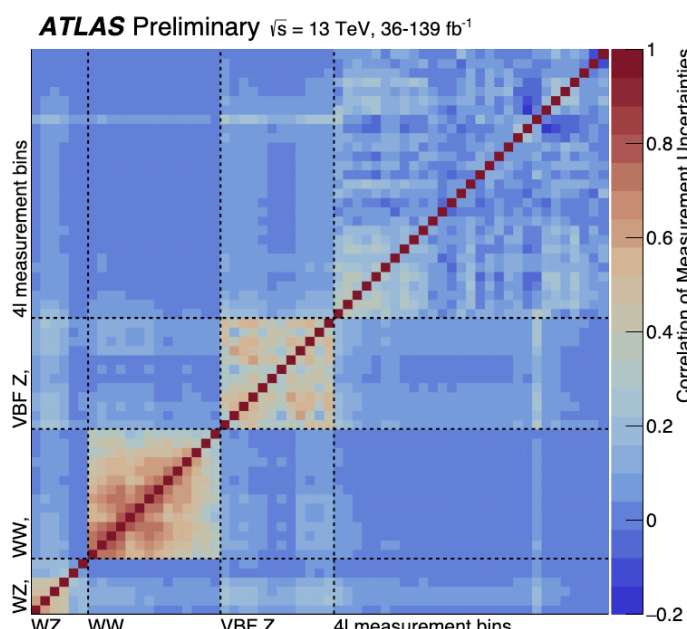


Process	Important phase space requirements
$pp \rightarrow e^\pm \nu \mu^\mp \nu$	$m_{\ell\ell} > 55 \text{ GeV}$, $p_T^{\text{jet}} < 35 \text{ GeV}$
$pp \rightarrow \ell^\pm \nu \ell^\pm \ell^-$	$m_{\ell\ell} \in (81, 101) \text{ GeV}$
$pp \rightarrow \ell^+ \ell^- \ell^+ \ell^-$	$m_{4\ell} > 180 \text{ GeV}$
$pp \rightarrow \ell^+ \ell^- jj$	$m_{jj} > 1000 \text{ GeV}$, $m_{\ell\ell} \in (81, 101) \text{ GeV}$

Observable	$\mathcal{L} [\text{fb}^{-1}]$
$p_T^{\text{lead. lep.}}$	36
m_T^{WZ}	36
m_{Z2}	139
$\Delta\phi_{jj}$	139

- ATLAS electroweak data
- Differential cross-section measurements for diboson and Z production via VBF

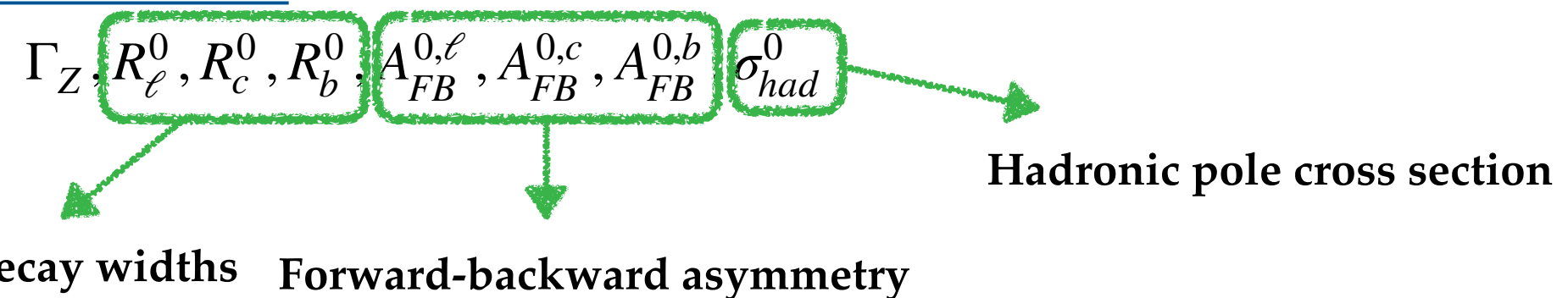
SMEFTsim: “topU3l” flavour symmetry”



First ATLAS Global combination

Precision Electroweak Measurements

on the Z Resonance



- Tight limit provided by LEP-> only sensitive to a limited number of parameters.
- Parametrisation of EW pole observables only in the linear approximations:
 - Two different fit setups: Higgs+EW and Higgs+EW+EWPO
- The likelihood is modelled as a multivariate Gaussian, both theoretical and experimental uncertainties are included in the covariance matrix.

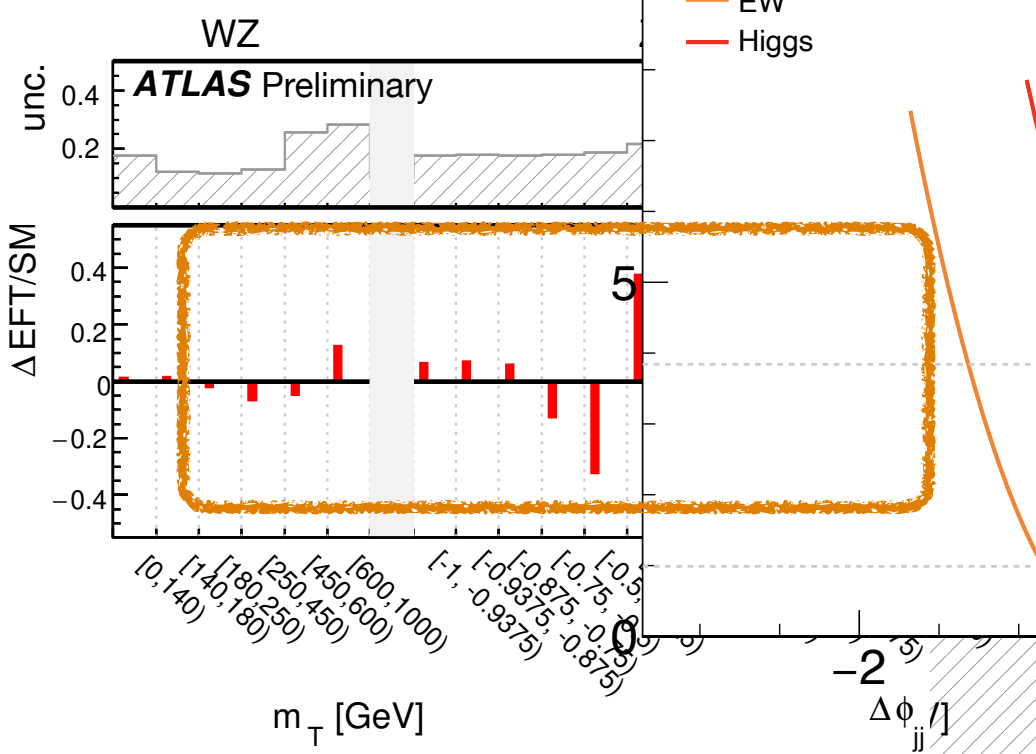
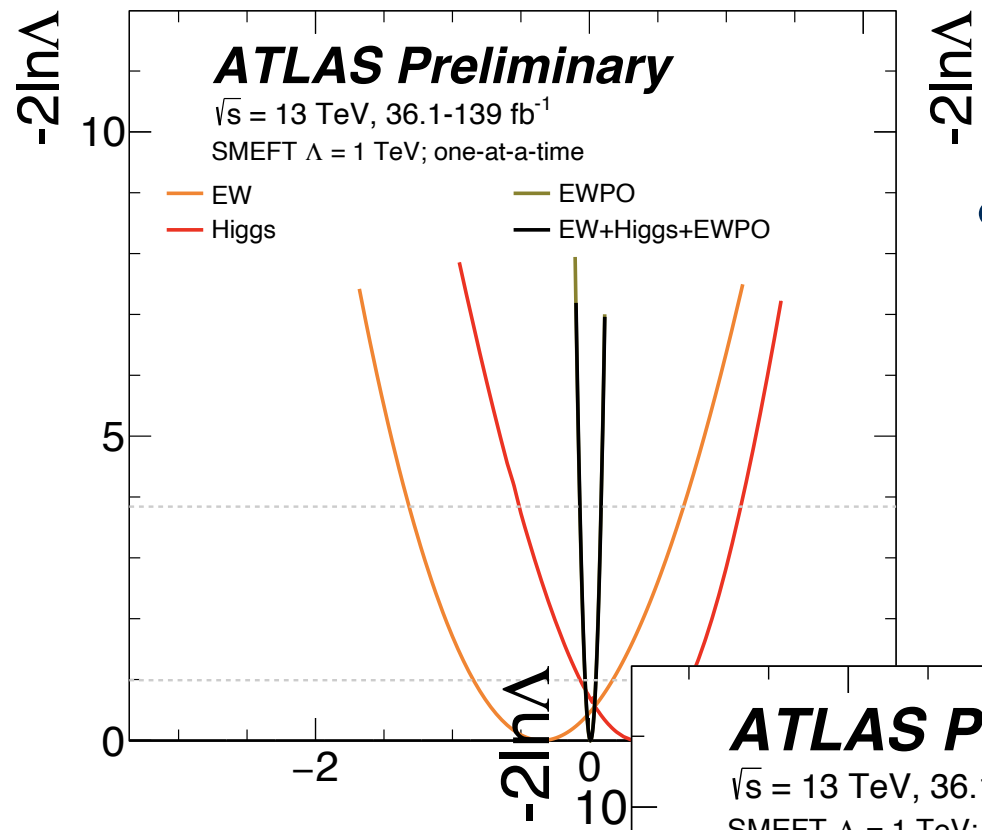
EWPD in the SMEFT to dimension eight

Observable	Measurement	Prediction	Ratio
Γ_Z [MeV]	2495.2 ± 2.3	2495.7 ± 1	0.9998 ± 0.0010
R_ℓ^0	20.767 ± 0.025	20.758 ± 0.008	1.0004 ± 0.0013
R_c^0	0.1721 ± 0.0030	0.17223 ± 0.00003	0.999 ± 0.017
R_b^0	0.21629 ± 0.00066	0.21586 ± 0.00003	1.0020 ± 0.0031
$A_{FB}^{0,\ell}$	0.0171 ± 0.0010	0.01718 ± 0.00037	0.995 ± 0.062
$A_{FB}^{0,c}$	0.0707 ± 0.0035	0.0758 ± 0.0012	0.932 ± 0.048
$A_{FB}^{0,b}$	0.0992 ± 0.0016	0.1062 ± 0.0016	0.935 ± 0.021
σ_{had}^0 [pb]	41488 ± 6	41489 ± 5	0.99998 ± 0.00019

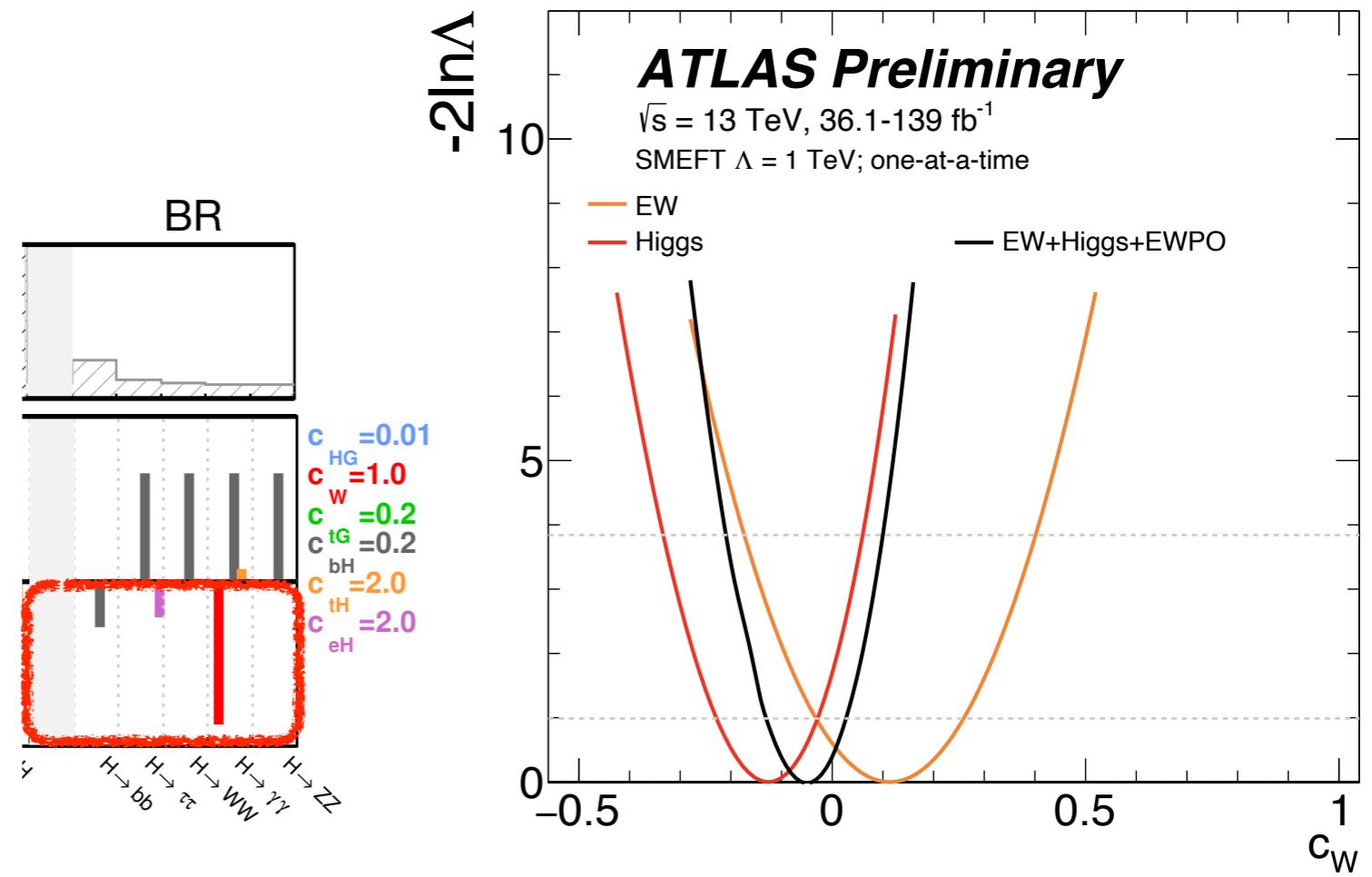
- Electroweak precision observables measured at LEP and SLC
- Eight pseudo observables describing the physics at the Z-pole are interpreted.
- Measurement probed with high sensitivity O(1 - 0.01 %)

ATLAS Global combination: one at a time

[ATL-PHYS-PUB-2022-037](#)



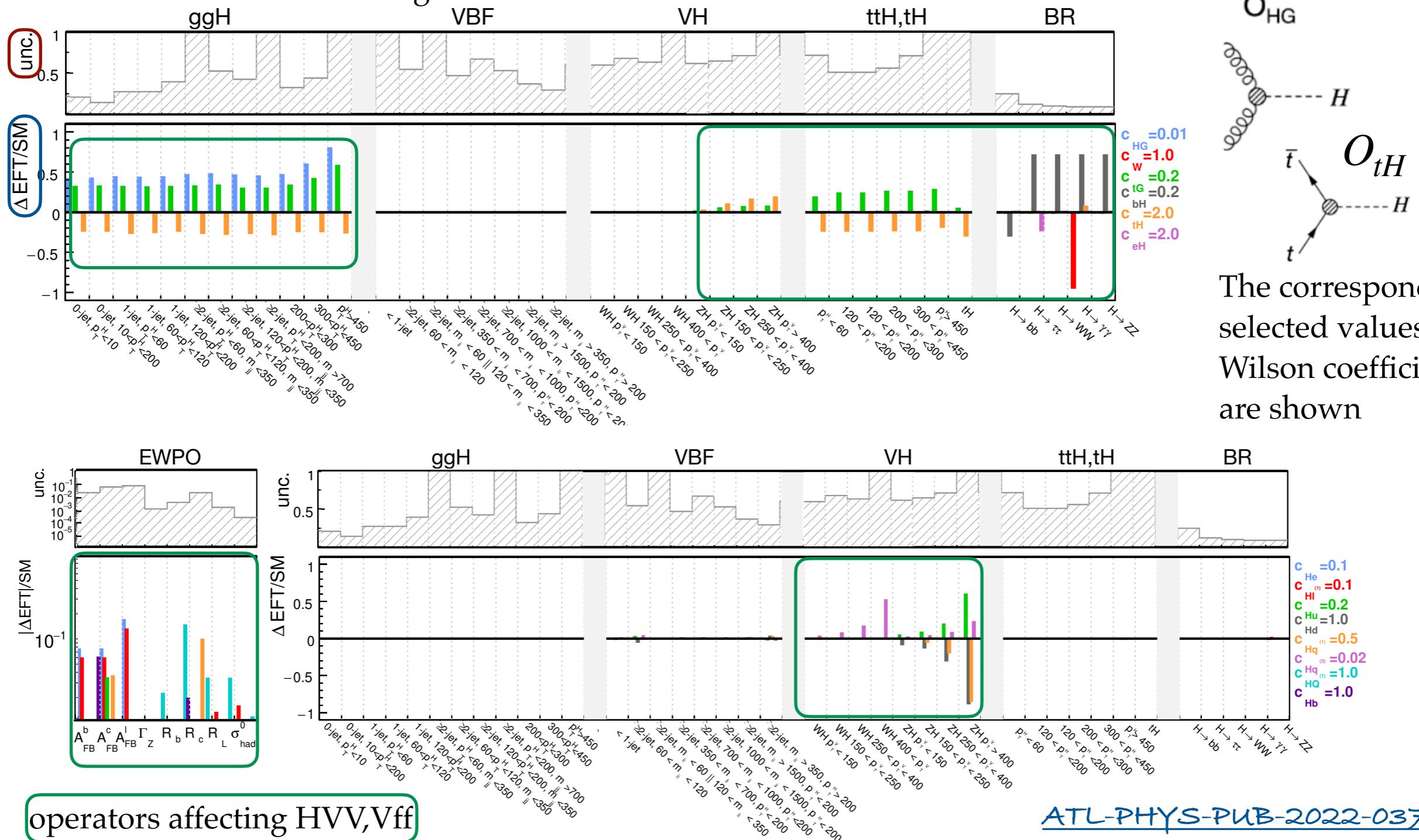
- One parameter at a time scans to compare sensitivity to an operator across the 3 measurement groups;
 - all remaining Wilson coefficients fixed to zero;
 - correlations between operators are neglected.



ATLAS Global combination

Impact of linear SMEFT parameterisation shown for bins along with corresponding measurement uncertainty

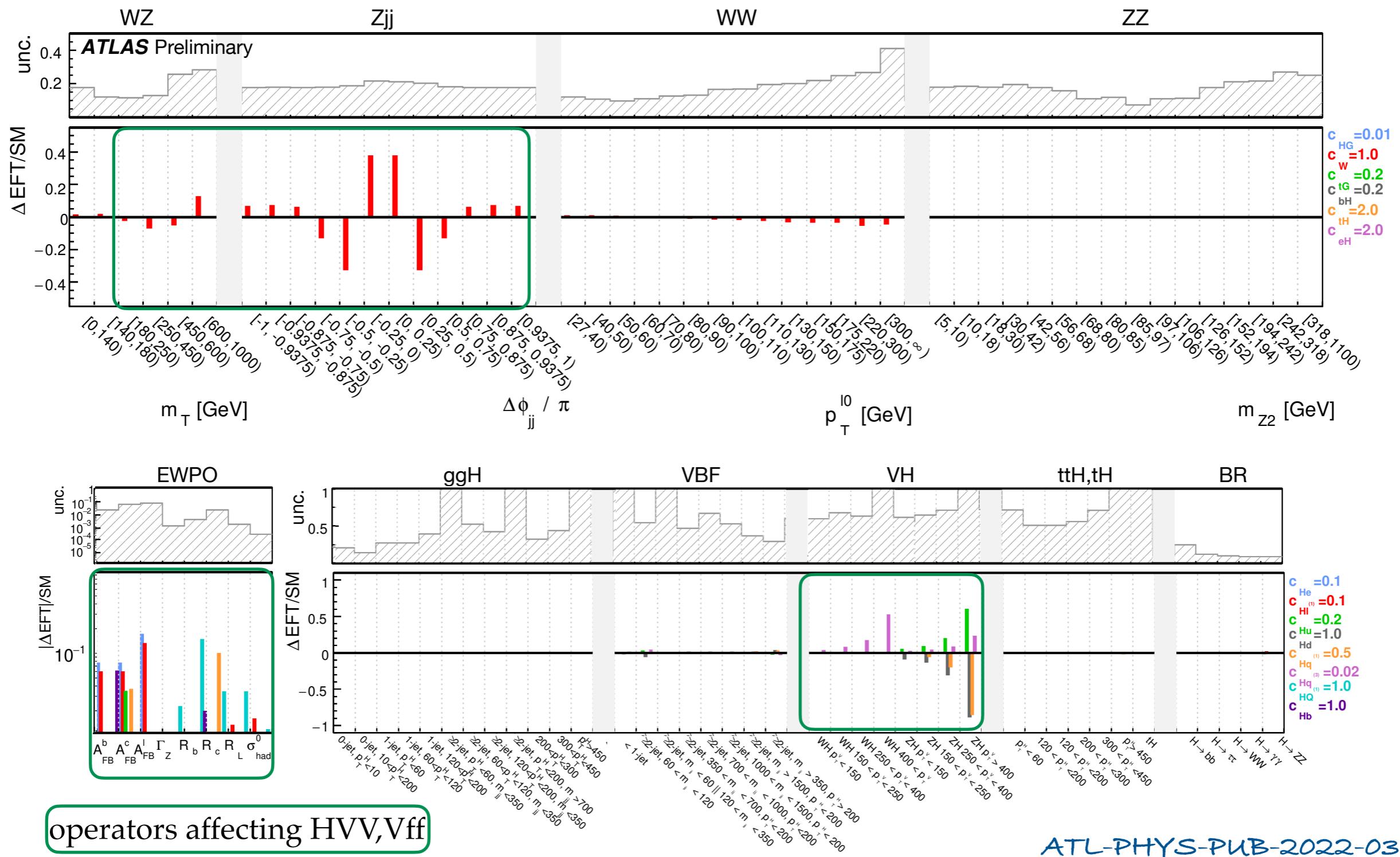
- Relative impact of linear SMEFT terms with Wilson coefficients c_{HG} , c_W , c_{tG} , c_{bH} , c_{tH} , and c_{eH} on the Higgs STXS cross sections and branching ratios.



ATL-PHYS-PUB-2022-037

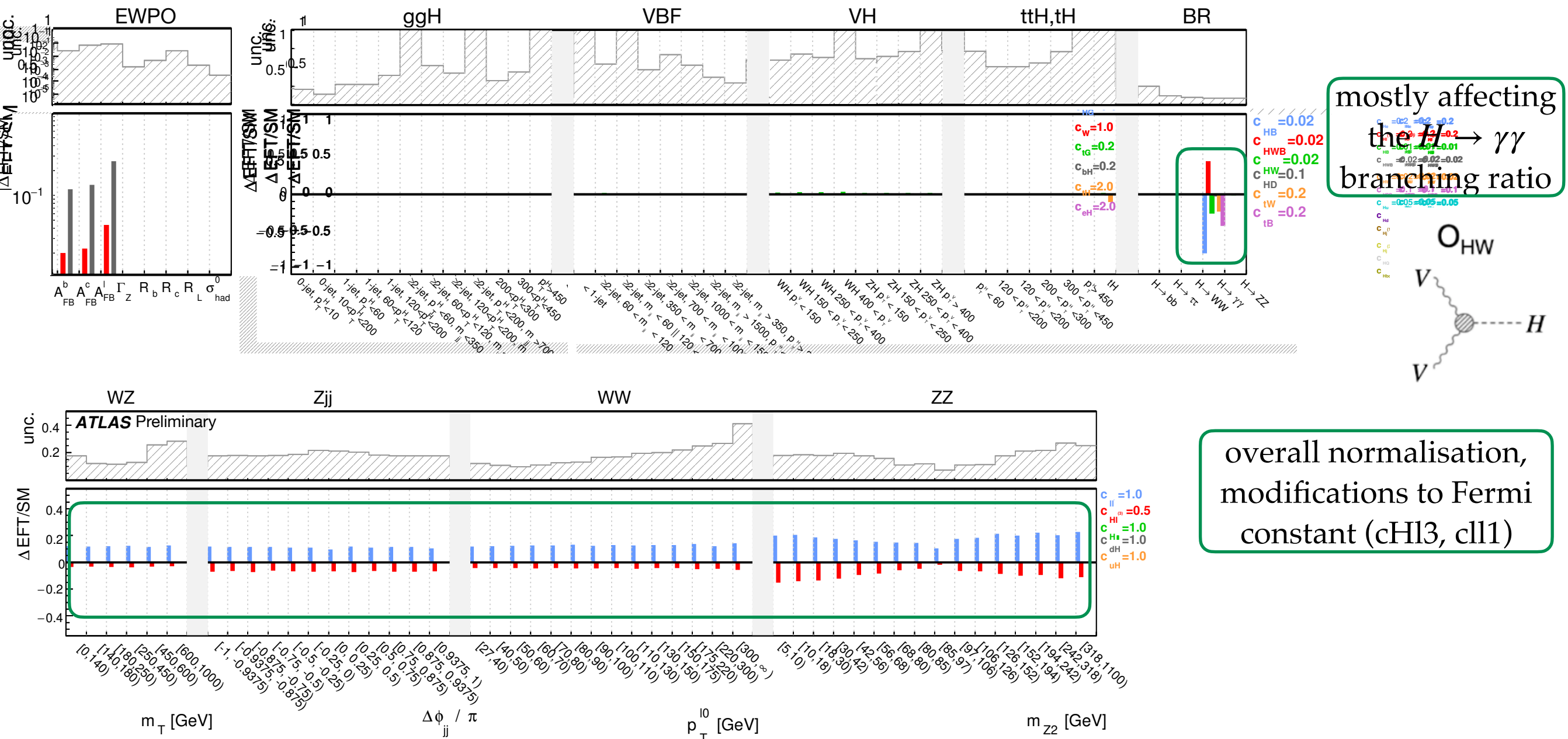
ATLAS Global combination

- Additional sensitivity coming from EW measurements and EWPO, e.g. cW that cannot be disentangled using just $H \rightarrow \gamma\gamma$ decay.



ATLAS Global combination

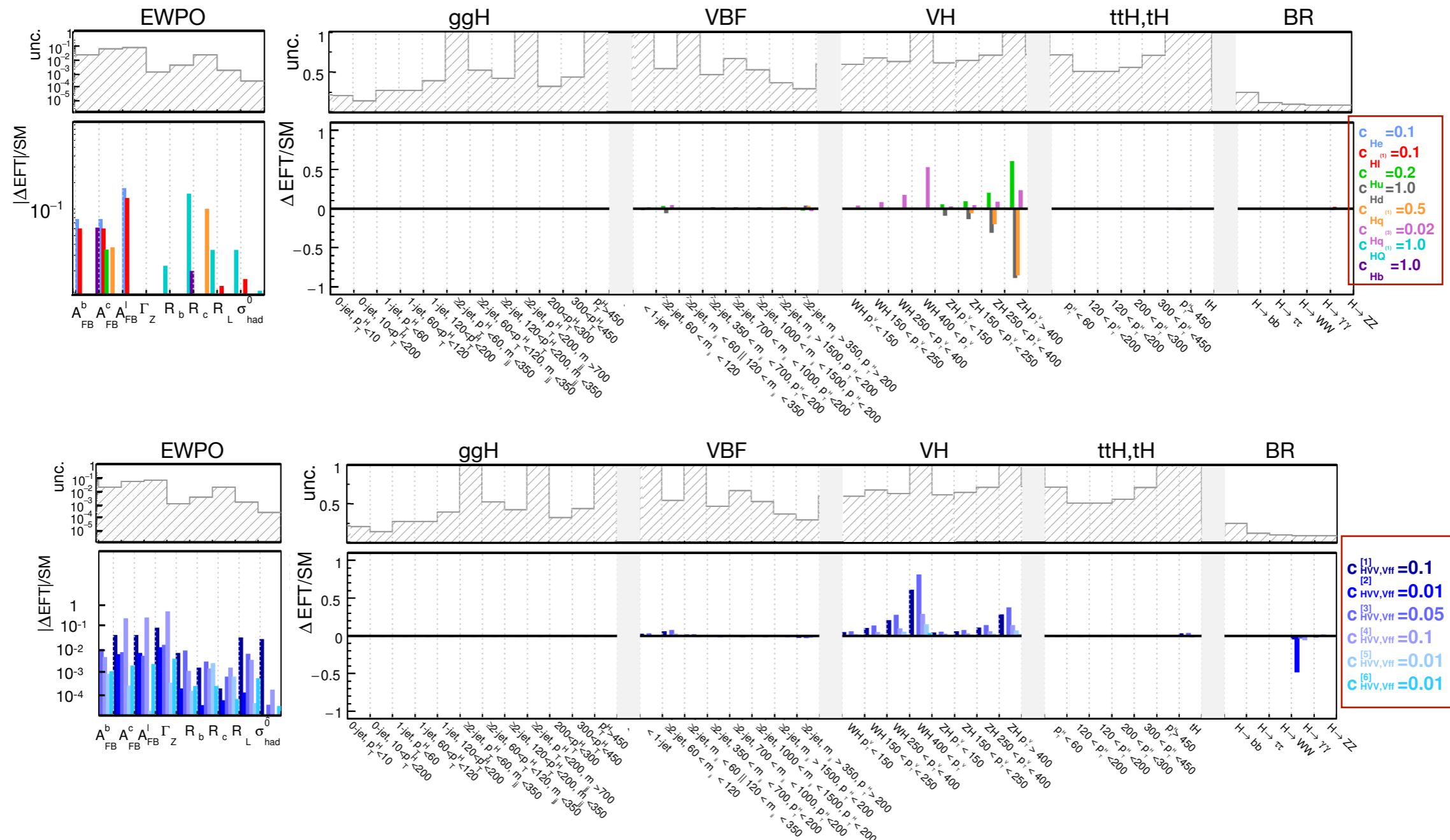
Impact of linear SMEFT parameterisation shown for bins along with corresponding measurement uncertainty



ATL-PHYS-PUB-2022-037

ATLAS Global combination

- SMEFT impact on measurements shown in Warsaw basis and fit basis-> allows to understand the impact of the different fit directions on measurements.



ATLAS Global combination: statistical combination

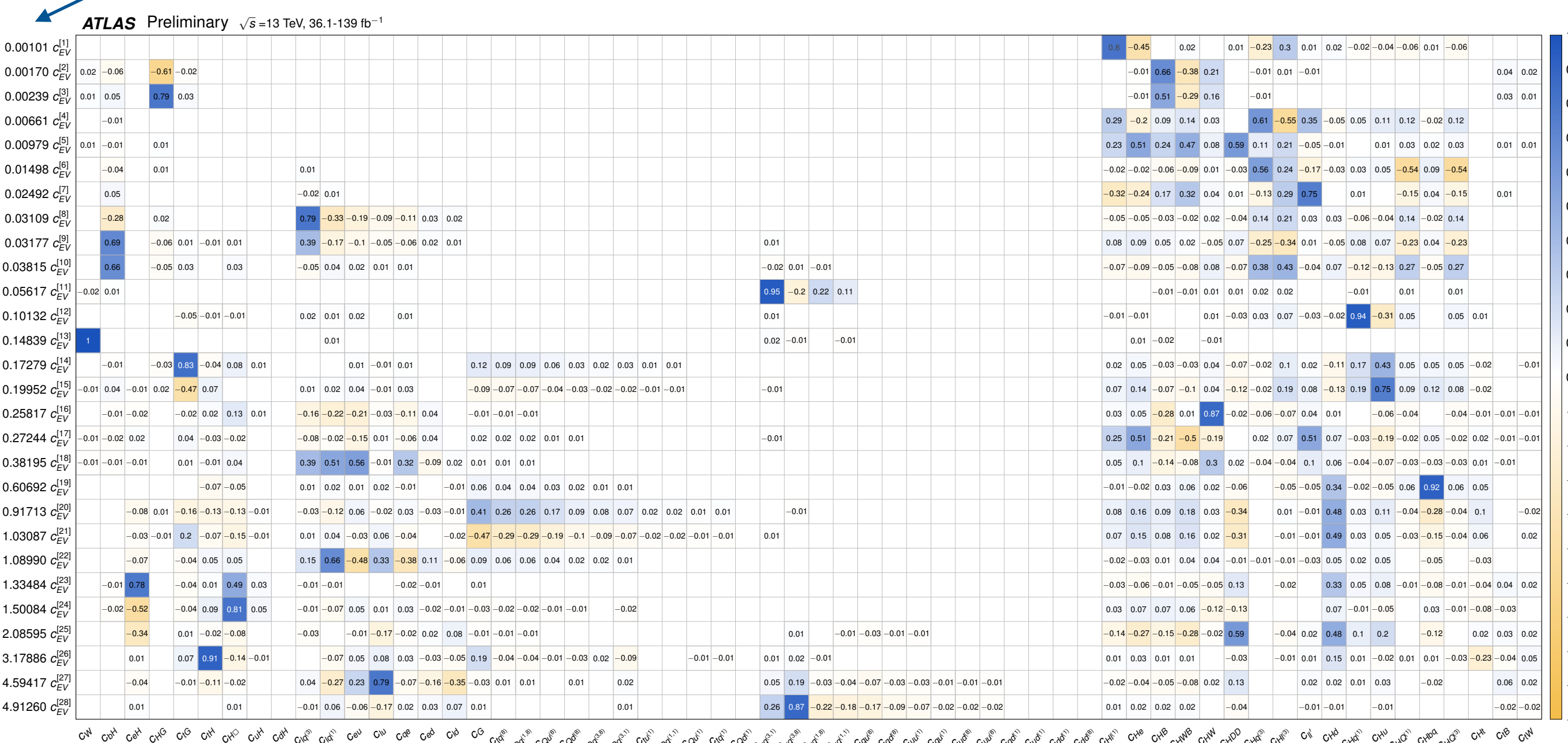
- Overlapping categories:
 - regions of the inclusive 4ℓ analysis that target $m_{4\ell} < 180 \text{ GeV}$ are excluded (small impact on SMEFT).
 - the 0-jet WW control region from HWW is excluded; WW normalisation is correlated with WW signal normalisation.
- A multivariate Gaussian model is used for the interpretation of both LHC EW measurements and EWPO.
- Systematic uncertainties modelled with common nuisance parameter:
 - for unfolded SM measurements: experimental nuisance parameter shift unfolded results;
 - same nuisance parameter shift reco-level prediction for Higgs measurements.
- For EWPO the model contains no nuisance parameters and both theoretical and experimental uncertainties are included in the covariance matrix.
- Limits on WCs extracted using combined likelihood (product of individual likelihood).

Correlated Uncertainty Source	Parameters
Luminosity (correlated part)	1
Luminosity 2015/16	1
Luminosity 2017/18	1
Pile-up modelling	1
Pile-up jet suppression	1
Jet energy scale (pile-up modelling)	3
Jet energy scale η -inter-calibration	1
Jet energy resolution	12
B-tagging efficiency (WW and $H \rightarrow WW^*$)	1
WW modelling (WW and $H \rightarrow WW^*$)	2

ATLAS Global combination: sensitivity studies

- PCA considering all operators: directions ordered by increasing uncertainties, keeping $\sigma < 5$;
 - Wilson coefficients expected to be at most order 1, new physics scale Λ expected to be at least 1 TeV -> directions with $\sigma > 5$ have very little impact on the measurement.

Eigenvectors from PCA, corresponding eigenvalues

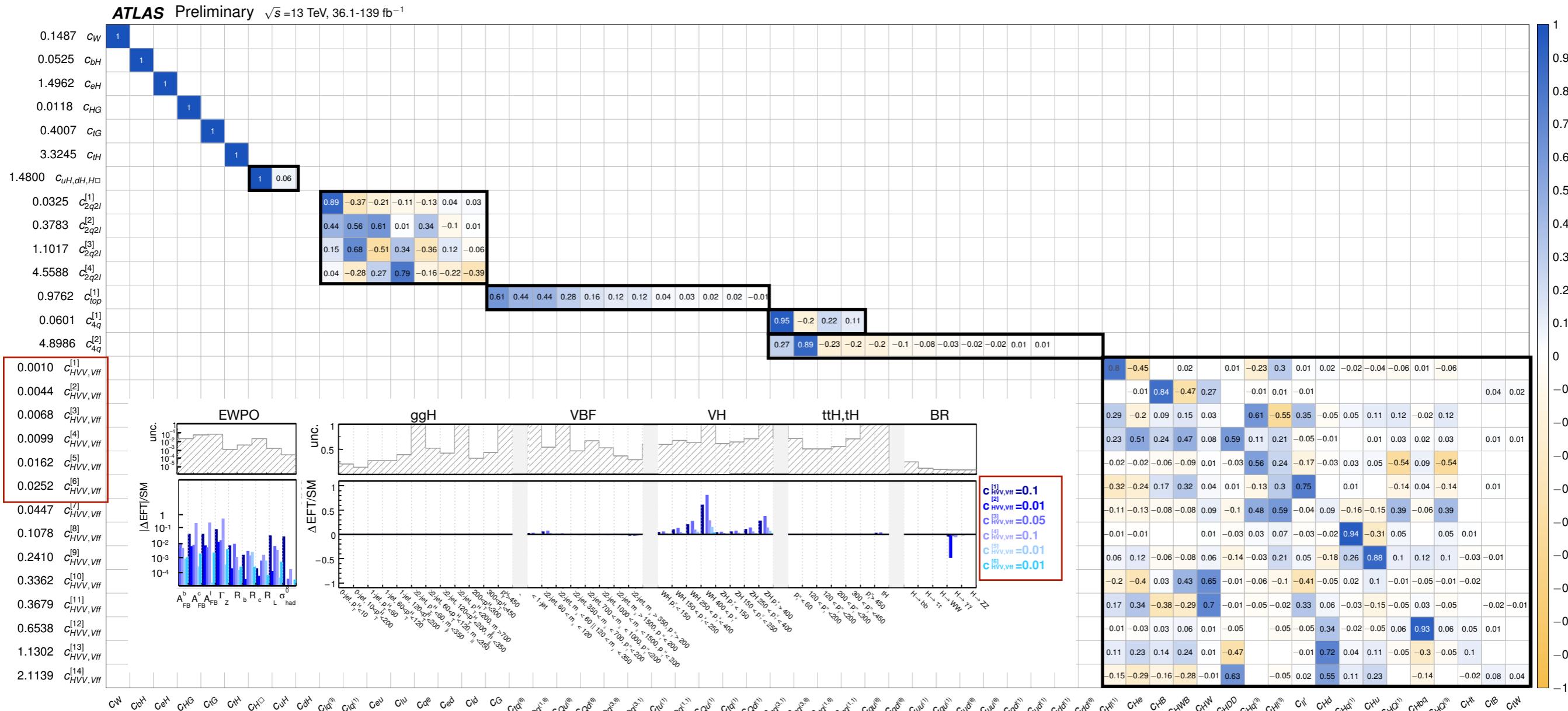


ATL-PHYS-PUB-2022-037 Warsaw Basis, Wilson coefficients



ATLAS Global combination: sensitivity studies

- PCA considering all operators: directions ordered by increasing uncertainties, keeping $\sigma < 5$;
 - Fit basis defined by grouping operators of similar physics impact together.



Warsaw Basis, Wilson coefficients

ATLAS Global combination: simplified likelihood

ATL-PHYS-PUB-2022-037

- Simplified likelihood model:
 - format to deliver results for re-interpretation;
 - signal strength modifier + correlation matrix.
- Results from the full likelihood fit compared to those using a simplified likelihood following a multi-variate Gaussian approach:
 - minimal differences between the two methods;
 - the simplified model is nuisance parameter free, as the effect of all uncertainties is encoded in the covariance matrix-> computationally inexpensive.
- Signal strength modifiers + correlation matrix available, preparing shared parameterisation.

